



REVIEW ARTICLE

Mass spectrometry imaging: new eyes on natural products for drug research and development

Jin-jun Hou^{1,2}, Zi-jia Zhang^{1,2}, Wen-yong Wu^{1,3}, Qing-qing He¹, Teng-qian Zhang^{1,2}, Ya-wen Liu^{1,2}, Zhao-jun Wang^{1,2}, Lei Gao^{1,2}, Hua-li Long^{1,2}, Min Lei^{1,2}, Wan-ying Wu^{1,2} and De-an Guo^{1,2}

Natural products (NPs) and their structural analogs represent a major source of novel drug development for disease prevention and treatment. The development of new drugs from NPs includes two crucial aspects. One is the discovery of NPs from medicinal plants/microorganisms, and the other is the evaluation of the NPs in vivo at various physiological and pathological states. The heterogeneous spatial distribution of NPs in medicinal plants/microorganisms or in vivo can provide valuable information for drug development. However, few molecular imaging technologies can detect thousands of compounds simultaneously on a label-free basis. Over the last two decades, mass spectrometry imaging (MSI) methods have progressively improved and diversified, thereby allowing for the development of various applications of NPs in plants/microorganisms and in vivo NP research. Because MSI allows for the spatial mapping of the production and distribution of numerous molecules in situ without labeling, it provides a visualization tool for NP research. Therefore, we have focused this mini-review on summarizing the applications of MSI technology in discovering NPs from medicinal plants and evaluating NPs in preclinical studies from the perspective of new drug research and development (R&D). Additionally, we briefly reviewed the factors that should be carefully considered to obtain the desired MSI results. Finally, the future development of MSI in new drug R&D is proposed.

Keywords: natural product; mass spectrometry imaging; MALDI; DESI; molecular imaging; ion mobility

Acta Pharmacologica Sinica (2022) 43:3096–3111; <https://doi.org/10.1038/s41401-022-00990-8>

INTRODUCTION

Natural products (NPs) represent an important source of novel drugs. Approximately 23.5% of FDA-approved drugs are derived from NPs or their derivatives, most of which are used for antibacterial and anticancer therapies [1]. In China, more new drugs, including drugs based on traditional Chinese medicine (TCM), have been obtained from NPs [2, 3], such as artemether [4], huperzine A [5], *Salvia miltiorrhiza* depside salt [6], etc. To develop new drugs from NPs, the first step is to extract and screen NPs from organisms (such as medicinal plants/microorganisms). However, obtaining or discovering NPs from medicinal plants or microorganisms is still difficult [7]. Preclinical studies represent one of the most crucial stages in new drug development; however, current preclinical drug evaluations largely fail to satisfy the drug development demand. New preclinical strategies are being adopted to augment the predictive values of in vivo studies [8]. The heterogeneous spatial distribution of NPs in medicinal plants/microorganisms [9] or tumor models [10] can provide valuable information for drug development (Fig. 1). Many thrilling molecular imaging technologies have been applied to discover NPs or facilitate preclinical studies, such as radiographic imaging like positron emission tomography (PET) and single photon emission computed tomography (SPECT), magnetic resonance imaging (MRI), computed tomography (CT), fluorescence imaging,

and Raman imaging [11] (Table 1); however, few molecular imaging technologies can detect thousands of molecules simultaneously on a label-free basis.

Mass spectrometry imaging (MSI) technology can spatially map the production and distribution of molecules in situ without labeling, thereby providing a flexible approach for directly investigating biological samples to identify both known and unknown molecular features [12, 13]. MSI can provide thousands of molecular images in plants, animals, and microbes, including elements, small molecules, lipids, oligosaccharides, peptides, and native proteins. Over the last two decades, MSI methods have progressively improved and their ionization methods, sensitivity, and spatial resolution have diversified; thus, they have been widely used to identify NPs from medicinal plants/microorganisms [13–22] and develop novel therapies [22–41]. Such tools provide new visualization methods for natural product research. In this mini-review, we will focus on MSI applications to discover NPs from medicinal plants to determine how NPs are produced and evaluate NPs in in vivo studies to identify their mechanisms from a new drug research and development (R&D) perspective (Fig. 1). Hopefully, data on NPs provided by MSI technology will hopefully lead to breakthroughs in new drug development. Additionally, the MSI method is usually composed of four steps: sample preparation, ionization in situ, mass spectrometry acquisition, and

¹National Engineering Research Center of TCM Standardization Technology, Shanghai Institute of Materia Medica, Chinese Academy of Sciences, Shanghai 201203, China;

²University of Chinese Academy of Sciences, Beijing 100049, China and ³School of Chinese Materia Medica, Nanjing University of Chinese Medicine, Nanjing 210029, China

Correspondence: Wan-ying Wu (wanyingwu@simm.ac.cn) or De-an Guo (daguo@simm.ac.cn)

These authors contributed equally: Jin-jun Hou, Zi-jia Zhang

Received: 13 June 2022 Accepted: 25 August 2022

Published online: 13 October 2022

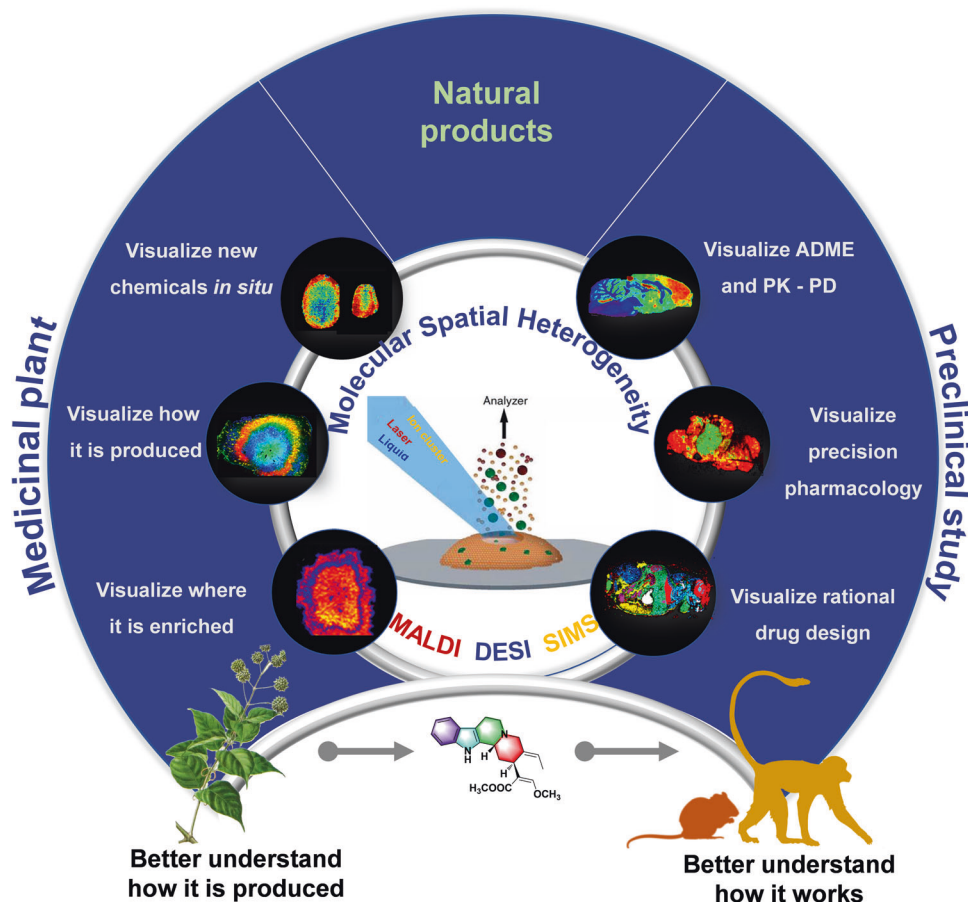


Fig. 1 Mass spectrometry imaging can facilitate the discovery of NPs and its preclinical study by visualizing the molecular spatial heterogeneous spatial distribution in medicinal plant and in vivo.

Table 1. Pros and Cons of MSI with other molecular imaging technologies [11].

Technologies	Research object	Spatial resolution	Analytes	Analytes number	Sensitivity	Analysis time
MSI	Tissue slide	Middle resolution (1 ~100 μm)	Unlabeled	Thousands	Middle	Slow
FI	Tissue slide whole body	High resolution (subcellular level)	Labeled	A few	High	Middle
RSI	Tissue slide whole body	High resolution (cellular level)	Unlabeled /labeled	A few	Middle	Slow
MRI	Whole body	Low resolution (0.5–2 mm)	Unlabeled	H-atom	Low	Middle
PET	Whole body	Low resolution (1–2 mm)	Radiolabeling	A few	Low	Middle

FI fluorescence imaging, RSI Raman scattering imaging, MRI magnetic resonance imaging, PET positron emission tomography.

molecular imaging analysis. The most crucial steps are sample preparation [12, 14, 32] and in situ ionization [13], which includes matrix-assisted laser desorption/ionization (MALDI) [42], desorption electrospray ionization (DESI) [33], and secondary ion mass spectrometry (SIMS) [43, 44]. Many contributing factors should be carefully considered to obtain the desired MSI results. The critical aspects that must be focused on in experiments are also briefly reviewed.

MSI CAN FACILITATE THE DISCOVERY OF NPS BY VISUALIZING THEIR HETEROGENEOUS DISTRIBUTION IN MEDICINAL PLANTS

NPs mainly come from secondary metabolites and some primary metabolites of medicinal plants/microorganisms, and the distribution of NPs in a medicinal plant is usually heterogeneous. With MSI technology, it is possible to visualize the primary and secondary

metabolites to study their spatial distribution heterogeneity in medicinal plants, which is conducive to better discovering novel NPs for new drug development. NP discovery is mainly performed to achieve the following three objectives [14, 17, 18]: to optimize the extraction method of NPs, MSI techniques can be applied to locate the parts in the medicinal plant where NPs are enriched; to improve the production of NPs in medicinal plants, MSI techniques provide a better understanding of the NP biosynthesis process; and to discover novel NPs, MSI techniques can reveal hidden or unstable NPs.

MSI helps locate the parts of medicinal plants where NPs are enriched to optimize the extraction method. The heterogeneous distribution of NPs in medicinal plants is related to their botanical structures. Traditional analytical techniques, such as liquid chromatography–mass spectrometry (LC–MS), can only

analyze and characterize the NPs from medicinal plants in different plant parts separately, such as the roots, stems, and leaves. Locating the distribution of NPs with the corresponding botanical structures is difficult, which hinders the collection of useful information for improving processing or extraction methods. MSI technology has the advantages of being label-free and providing high spatial resolution images, which enables the analysis of the spatial distribution of NPs in medicinal plants and colocalization of NPs with their botanical structures, thereby providing information improving NP extraction methods. Over the past five years, a variety of medicinal plants have been studied using MSI techniques, including *Vitex agnus-castus* L. (Sui-Hua-Mu-Jing) [45], *Ginkgo biloba* (Yin-Xing) leaves [46], *Hypericum perforatum* (Guan-Ye-Jin-Si-Tao) roots [47], agarwood (Chen-Xiang) [48], *Curcuma longa* (Jiang-Huang) [49], *Catharanthus roseus* (Chang-Chun-Hua) leaves [50], *Salvia miltiorrhiza* Bge (Dan-Shen) [51, 52], *Sassafras albidum* (Bei-Mei-Cha-Shu) [53], *Paeonia suffruticosa* (Mu-Dan), *Paeonia lactiflora* (Shao-Yao) [54], *Panax notoginseng* (San-qi) [55], *Clausena lansium* (Lour.) skeels (Huang-pi) [56], *Panax ginseng* (Ren-Shen) [57], *Lycium barbarum* L. (Gou-Qi-Zi) [58], *Dallopia multiflora* (Thunb.) Harald. (He-Shou-Wu) [59], *Prunus persica* (L.) Batsch (Tao-Ren) seeds, *Prunus aymeniaca* L. var. *ansu* Maxim (Ku-Xing-Ren), and *Prunus humilis bunge* (Yu-Li-Ren) [60].

For example, paeoniflorin and its derivatives, which are as the characteristic components in the medicinal plants of the genus *Paeonia*, are found in the roots of *P. suffruticosa* (PS) and *P. lactiflora* (PL). However, their spatial distribution in the root is still unknown. Therefore, two MSI platforms, MALDI fourier transform ion cyclotron resonance MS (MALDI-FT-ICR-MS) and atmospheric-pressure-scanning microprobe MALDI-quadrupole-Orbitrap (AP-SMALDI-Q-Orbitrap), were used to perform a comparative analysis of the two roots using transverse sections at 35 $\mu\text{m} \times 35 \mu\text{m}$ spatial resolution. In this study, approximately 65 secondary metabolites were identified by the investigators, and their spatial distribution had significant differences in the cork, cortex, phloem, and xylem parts, corresponding to the root sections of PS and PL. Among them, the abundance of paeoniflorin, one of the primary natural products in the roots of PS, was approximately two to five times higher than that in PL, and its distribution in phloem was significantly higher than that in the xylem of PS (Fig. 2a). Therefore, when using the roots of PS for therapeutic purposes as a TCM, its xylem is often removed to increase the relative content of paeoniflorin. In addition, it was found that the cortex of PL roots is particularly enriched in certain compounds, including ebenzoylpaeoniflorin, oxypaeoniflorin, and benzoylpaeoniflorin. However, when PL is used in the TCM Bai-Shao (*Paeoniae Radix Alba*), the cortex needs to be removed, indicating that these compounds might not contribute much to its therapeutic effects [54]. A similar approach was adopted to study the roots of *Panax notoginseng*. The MALDI-TOF/TOF-MSI platform was adopted, and the results showed that different parts of *Panax notoginseng* roots, such as the rhizome, main roots, and branch roots, presented differences in the abundance of dencichine, which is the primary hemostatic compound synthesized in *Panax notoginseng* [55]. Thus, the results obtained using MSI technology provide useful information to select the appropriate parts of the medicinal plants to extract the desired NPs (Fig. 2d).

Amygdalin is a characteristic compound in the seeds of peach, bitter almond, and Chinese dwarf cherry. Our research group used the DESI-ion mobility-quadrupole time-of-flight (DESI-IM-QTOF) MSI platform to analyze the spatial heterogeneity of the three medicinal seeds at a spatial resolution of 100 $\mu\text{m} \times 100 \mu\text{m}$. The spatial distribution of nearly 80 primary and secondary metabolites was analyzed, including the unique compound amygdalin, oligosaccharides, glycerides, and glycerol phospholipids, and most were more abundant at the edge of the seed kernel than in the center of the cotyledons. At the same time, lysophosphatides, which are hydrolyzed glycerol phospholipids that lose a fatty acyl

group, presented higher abundance in the center of the cotyledons [60] (Fig. 2b). These results provide hints for selecting suitable extraction methods to obtain NPs. For example, for bitter almond seeds, care should be taken to avoid soaking the seeds too long to prevent the hydrolysis of amygdalin around the outer area of the seeds.

MSI provides insights on the biosynthesis of NPs for improving NP production from medicinal plants

The production of NPs in medicinal plants is affected by their biosynthetic pathway and interactions between plants and the surrounding environment, which could change the efficiency of producing such compounds. Studies on these two factors could identify methods of increasing the biosynthesis and production of particular NPs. MSI can play a better role in exploring both aspects. For example, phenolic acids and tanshinones are the two main types of active NPs in *Salvia miltiorrhiza* Bge (Dan-shen). The DESI-QTOF MSI platform showed that the salvia phenolic acids were distributed throughout the above and underground parts of the plant while the tanshinones were only enriched in the pericardial tissue of the salvia root (Fig. 2c). Further analysis combined with nontargeted metabolomics based on LC-MS technology found that rosmarinic acid is at the center of the biosynthetic pathway of salvia phenolic acids, and the biosynthesis of rosmarinic acid based on danshensu and caffeic acid is the main pathway for *Salvia* plants. Tanshinones may be critical secondary metabolites, and their distribution in the underground roots helps the salvia plant resist environmental pathogens and damage [52]. MSI results indicated that increasing caffeic acid and danshensu should be useful for increasing the production of salvia phenolic acids. Moreover, pesticides should be reduced to increase the production of tanshinones. A similar approach was adopted in another study using the same MSI platform to investigate the changes in phytohormones in *Arabidopsis* leaves after mechanical damage. Phytohormones, including jasmonates, salicylic acid, abscisic acid, and indole-3-acetic acid [61], were evaluated by MSI (Fig. 2e), and the results showed that these phytohormones were significantly increased in the damaged areas of the leaves. Overall, these studies provided valuable information to increase the production of NPs in medical plants.

MSI helps reveal hidden or unstable NPs for novel drug development

MSI may reveal novel NPs that are overlooked using classic LC-MS techniques [14] because after pulverizing and extracting, some NPs may be masked by compounds with high abundance or change during the sample preparation process. Analyzing tissue sample sections in situ makes it possible to detect and discover new compounds due to their natural enrichment in their native location in the tissue [14]. For example, to discover new antibiotics from bacterial colonies, the secondary metabolites of a kind of actinobacteria were mapped with the DESI-MSI platform. This technology was able to identify an m/z 1299 ion on the glass slide only and not by using the imprint method. Further observation of the spatiotemporal distribution of the ion revealed that it was only synthesized by healthy young cells of the bacterial colony. Moreover, the novel identified compound was presumed to be an analog of the antifungal agent lienomycin [62]. In this study, the MSI technique showed unmatched power in discovering hidden NPs from the medicinal plant in situ. Our research group identified a phospholipid, phosphatidylethanolamine (PE) 36:0, only in the fresh root section of *Rehmannia glutinosa* (Di-Huang) (Fig. 2f), further supporting that the MSI technique could help reveal unstable NPs in fresh medicinal plants. The application of MSI technology for the above three objectives represents intuitive analysis approaches for discovering NPs from medicinal plants, increasing NP production from medicinal plants, and revealing novel trace NPs in unique samples.

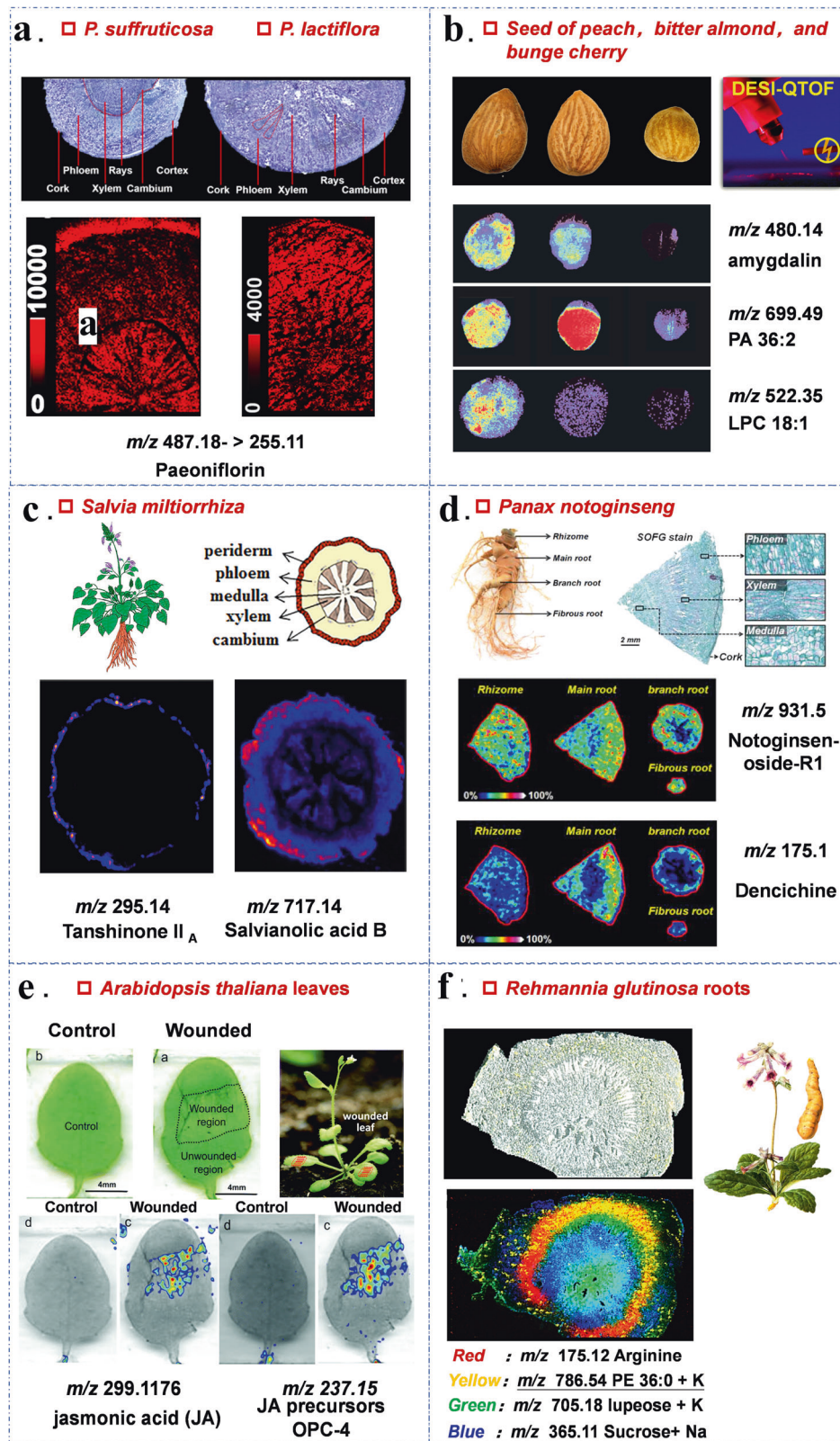


Fig. 2 Application of mass spectrometry imaging in discovery of natural products from medicinal plant /microorganisms. **a** MALDI-FT-ICR and AP-SMALDI-Q-Orbitrap MSI spatial distribution of secondary metabolites in the roots of *P. suffruticosa* (PS) and *P. lactiflora* (PL) [54], with permission from John Wiley & Sons. **b** DESI-IM-QTOF MSI spatial distribution of lipids in peach seed, bitter almond seed, and Chinese dwarf cherry seed [60], with permission from Elsevier. **c** DESI-QTOF MSI spatial distribution of secondary metabolites in *Salvia miltiorrhiza* Bge [52], with permission from Elsevier. **d** MALDI-TOF/TOF MSI spatial distribution of secondary metabolites in *Panax notoginseng* [55], under the terms of Creative Commons BY-NC-ND license. **e** DESI-QTOF MSI spatial distribution of phytohormones in *Arabidopsis* leaves after mechanical damage [61], with permission from Royal Society of Chemistry. **f** DESI-MSI spatial distribution of secondary metabolites in *Rehmannia glutinosa* roots (unpublished).

MSI CAN FACILITATE DRUG R&D BY VISUALIZING THE IN VIVO HETEROGENEOUS NP SPATIAL DISTRIBUTION

After bioactive NPs are obtained from medicinal plants/microorganisms, the MSI technique can be applied to promote preclinical studies based on the following three aspects [33]. First, in ADME (absorption, distribution, metabolism and excretion) and pharmacokinetic-pharmacodynamic (PK-PD) studies, MSI can provide the direct spatial distribution of compounds to facilitate more intuitive analyses of NPs and their ADME properties. Meanwhile, the spatial correlation between NPs and in situ endogenous pharmacodynamic biomarkers can be established. Second, in efficacy and safety evaluation and prediction studies, MSI technology enhances the accuracy and predictability of NP efficacy and toxicity analyses. Third, MSI can enhance the rationality of chemical modifications, formulation optimization, and nanomaterial selection for NP drug and preparation design.

MSI can improve the intuitiveness of ADME analysis and promote the spatiotemporal heterogeneity of drug PK-PD properties. In drug development, determining the drug's in vivo ADME is crucial to determining its drugability. Various molecular imaging techniques, including radiolabeling, magnetic resonance imaging, fluorescence imaging, and Raman imaging, have been used to study the tissue distribution of drugs [11, 30]. However, the MSI technique has unparalleled advantages in terms of retaining the spatial resolution and chemical features of NPs on a label-free basis [37].

First, the MSI technique can intuitively provide spatial heterogeneity information about chemicals without labeling. It has been used to study the distribution heterogeneity for certain NPs, such as YZG330/YZG331 [63], tetrandrine [64], paclitaxel [65], gis-soschizine methyl ether [66], scutellarin [67], and *Uncaria* tetracyclic indole alkaloids [68]. Since mass spectrometry results are susceptible to matrix effects, imaging data sometimes cannot directly reflect the actual in vivo distribution and concentration of NP molecules. To reflect the actual concentration of molecules in vivo, the quantitative spatial distribution of drugs or compounds must be realized through correction approaches [32], such as internal standard correction. At present, the quantitative application of MSI using correction approaches has been demonstrated to be well correlated and sometimes even comparable to the classic LC-MS technique, which can objectively reflect the distribution levels of drugs in tissues [32, 65, 69–81]. For example, using the quantitative DESI-QTOF MSI platform, our research group systematically studied the spatial distribution of seven characteristic tetracyclic monoterpene indole alkaloids in rat brain tissues. These indole alkaloids are considered bioactive compounds from *Uncaria* stems and hooks and commonly used in treating febrile seizures in TCM. The quantitative distribution was visualized, and the results showed that the seven tetracyclic monoterpene indole alkaloids have a significantly higher distribution in some circumventricular organs (CVOs), such as the pineal gland, area postrema (AP), and subcommissural organ (SCO) (Fig. 3a). *Uncaria* indole alkaloids were also highly distributed in the cerebral cortex, cerebellum, and hippocampal formation but showed a limited distribution in the pons, medulla oblongata, etc. Among them, the distribution of the three tetracyclic monoterpene indole alkaloids with smaller molecular polarity is significantly higher than that of the four tetracyclic monoterpenes oxidize indole alkaloids with greater polarity [68].

Second, MSI can intuitively display the spatial processes of drug absorption, which cannot be achieved by traditional analytical techniques. The dermal and intestinal absorption of drugs is the main factor for studying in vivo drug absorption. With the assistance of MSI technologies, the depth and extent of drugs absorbed via the dermis [30, 70, 79, 82–86] and intestines [76, 87] can be intuitively visualized and analyzed. For example, the MALDI-FT-ICR MSI platform showed that after focal administration

of tofacitinib in the intestine, its local concentration can be intuitively characterized by the gradual decline from the intestinal lumen to the proximal colonic muscle layer over time (Fig. 3b). Moreover, common saline flushing could not completely remove the drug from the lumen, which indicates that the traditional LC-MS method may overestimate the drug concentrations when analyzing intestinal tissue homogenates [76]. For the study of the dermal penetration property of compounds, the absorption kinetics process can be visualized in the initial few hours after topical bleomycin administration using the MALD-Q-Orbitrap imaging platform [86].

Third, MSI technology is conducive to evaluating the absorption characteristics of drugs in various compartments of the blood-brain barrier (BBB). The BBB has spatial heterogeneity in drug absorption capability. Using traditional analytical methods, only a limited number of brain regions can be divided and measured. MSI technology can achieve the fine distribution analysis of drugs in all brain regions simultaneously, thus leading to a better understanding of the effects of BBB characteristics on drug transport, including active transport, passive diffusion, and active efflux [75, 88]. In a neuro-PK study combined with MSI (Fig. 3c), the unloaded brain slices and those with saturated adsorption at constant blood concentrations in vitro were compared to explore the differences in the adsorption rate among various brain regions. By integrating the MALDI-FT-ICR MSI platform and quantitative imaging techniques, the blood-brain barrier absorption characteristics of olanzapine in different brain regions were achieved at a spatial resolution of 20 μm . The results showed that there was significant heterogeneity in BBB absorption among different brain regions. For example, BBB active efflux was most pronounced in the lateral septum region, where the striatum was characterized by passive diffusion and the anterior commissure region was characterized by active transport [75] (Fig. 3c).

Fourth, MSI technology can intuitively provide spatial distribution information for multiple metabolites simultaneously. For example, a study on gemcitabine, a prodrug to treat pancreatic cancer, was performed using the DESI-Q-Orbitrap and MALDI-FT-ICR platforms to simultaneously characterize the heterogeneous distribution of the original drug and its four metabolites in the tumor tissues (Fig. 3d). MSI analyses showed that the three metabolites of gemcitabine were mainly distributed in the areas where the tumor cells were highly active and showed a high abundance of AMP, ADP, and ATP. In contrast, the highest distribution of its original form and the inactive metabolite were different from the active metabolites. These results obtained using the MSI technique suggested that the production of active gemcitabine metabolites has a certain correlation with the activity of tumor cells [89].

Fifth, the MSI technique can simultaneously provide information about the spatial correlation of drug-induced pharmacodynamic biomarkers. The label-free feature of MSI makes it possible to visualize not only the spatial distribution characteristics of NPs and their metabolites with high spatial resolution but also the spatiotemporal changes in the corresponding endogenous pharmacodynamic biomarkers in vivo after drug intervention. For example, YGZ331/330 are a pair of epimer derivatives of N6-(4-hydroxybenzyl) adenine riboside (NHBA), a sedative and sleep-promoting compound isolated from *Gastrodia elata*. Using the AFADESI-Q-Orbitrap MSI platform, the in vivo distribution of YGZ331/330 was investigated at a spatial resolution of 400 μm . The MSI study revealed that the pair of epimers was mainly distributed in the stomach after oral administration. The main difference between the two epimers was that the metabolite of YGZ331 was rarely distributed in the stomach while the metabolite of YGZ330 had a significant presence in the gastric area. Further analysis was performed to analyze the spatial distribution of γ -aminobutyric acid (GABA) as the pharmacodynamic biomarker (Fig. 3e). Moreover, GABA in the YGZ330-treated

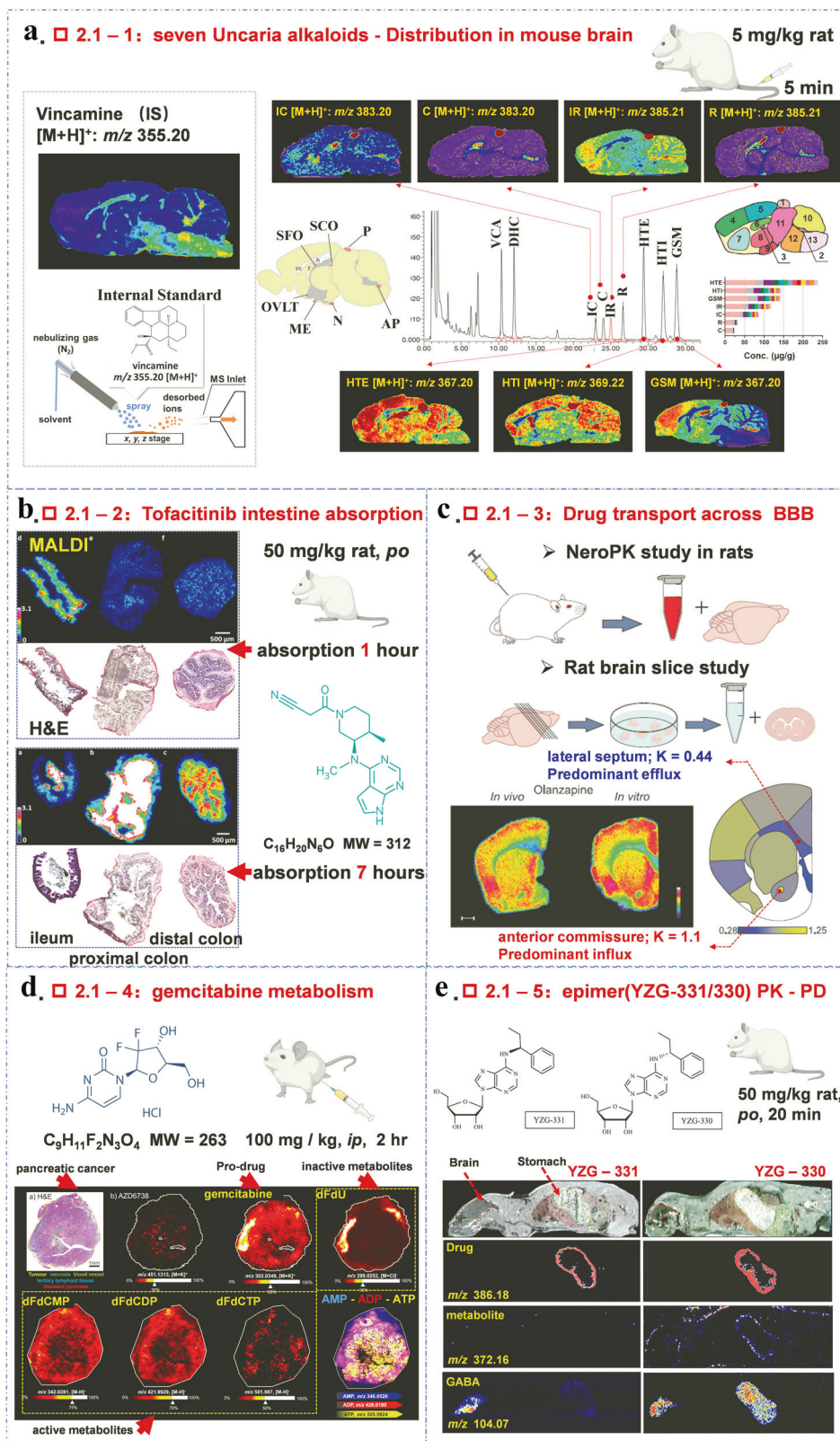


Fig. 3 Application of mass spectrometry imaging in ADME and PK-PD studies of drug development. a DESI-QTOF MSI spatial distribution of seven tetracyclic monoterpene indole alkaloids isolated from *Uncaria* stem with Hooks in mouse brain [68], with permission from Springer Nature. **b** MALDI-FT-ICR MSI spatial distribution of intestinal absorption of tofacitinib [76], with permission from American Chemical Society. **c** MALDI-FT-ICR MSI were adopted for evaluation of drug transport across BBB [75], under the terms of the Creative Commons CC BY license. **d** DESI-Q-Orbitrap and MALDI-FT-ICR MSI spatial distribution of gemcitabine and its four metabolites in pancreatic cancer [90], with permission from American Chemical Society. **e** AFADESI-Q-Orbitrap MSI spatial distribution of YZG331/330 with promoting sleep activity in the rat [63], under the Creative Commons CC-BY-NC-ND license.

group had the most significant increase in rat brain and gastric areas, which was consistent with the better efficacy of YGZ330 in terms of sedation and sleep promotion. These results suggest that differences in drug and their metabolite distribution may be related to endogenous pharmacodynamic biomarkers [63], which can be readily visualized with the assistance of MSI techniques.

MSI can promote the accuracy and predictability of NP efficacy and toxicity analysis

Uneven distribution of drugs can lead to “therapeutic heterogeneity” [29], particularly in the brain [68, 75, 88, 90–93], tumor tissues [89–91, 94–96], necrotic foci [97–100], gastrointestinal tracts [76], lymph nodes [101], etc. When the drug distribution heterogeneity is visualized in the target tissues at a high spatial resolution, the drug efficacy and toxicity assessment accuracy will be significantly improved, which may promote the ability to predict the potential efficacy or toxicity of drugs in their target organs. Thus, the concept of “precision pharmacology” has been developed and proposed by investigators [27].

First, analyzing the spatial heterogeneity of the drug distribution in target organs can improve our understanding of drug efficacy. For example, necrotic foci usually develop in tuberculosis tissues, and a small number of tuberculosis bacilli are wrapped inside the necrotic foci. With the MALDI-LTQ XL-Orbitrap imaging platform, five clinical anti-tuberculosis drugs were investigated. The results showed that only rifampicin was enriched in the lung necrotic foci after continuous administration, which effectively inhibited the tuberculosis bacteria inside the necrotic foci (Fig. 4a). This result indicated that rifampicin has long-term efficacy on tuberculosis; however, isoniazid, pyrazinamide, and moxifloxacin do not present this feature in treating tuberculosis [97]. The subsequent investigation applied the AP-MALDI-Q-Orbitrap MSI platform with a higher spatial resolution to further investigate the necrotic foci containing the tuberculosis bacteria. At a spatial resolution of 5 μm , it was confirmed that clofazimine could penetrate the tuberculosis granuloma. By combining this platform with the immunohistochemistry (IHC) technique, the colocalization of clofazimine with the penetrated macrophages was revealed. These results help better understand the pharmacodynamic mechanism of the drug for tuberculosis treatment [100].

Second, the drugs will lose their efficacy if they fail to achieve the ideal distribution at the target tissues or organs. For example, the distributions of antiretroviral drugs in the ileum of three species (mouse, macaque, and human) were explored using the infrared (IR)-MALDI-Q-Orbitrap platform. In combination with IHC and in situ hybridization using RNA viruses as probes, it was found that up to 27% of the cells infected by the viruses in ileum tissue were not exposed to antiretroviral drugs (Fig. 4b), which led to a small number of T cells remaining susceptible to viral infection and low-grade viral replication during antiretroviral suppression [101].

Third, the organs where the drug is distributed and enriched are closely related to its efficacy or toxicity. With further development of the MSI technique and improvements in the spatial resolution and sensitivity of the instruments, it is possible to predict the potential efficacy or toxicity of NPs based on the results of MSI analysis. For example, a previously mentioned study that explored the brain distribution of *Uncaria* indole alkaloids showed that their high distribution in CVOs provides a novel research direction to further explore their therapeutic potential in treating central nervous system (CNS) diseases. For toxicity prediction, the DESI-QTOF MSI platform showed that a chlorine-containing metabolite of diazepam was concentrated predominantly in the spinal cord of female zebrafish, suggesting that it may have sites of toxicity in the nervous system and exhibit sex differences [102]. Using the MALDI-TOF MSI platform, the spatial distribution of the antitumor drug MERTK (MER Proto-Oncogene, tyrosine kinase inhibitor) was explored at a spatial resolution of 10 μm . The results showed that the MERTK inhibitor was locally enriched in the retinal pigmented

epithelium and the site of retinopathy (Fig. 4c), suggesting that such drugs may have ocular safety risks. By revealing the correlation between the spatial distribution of the MERTK inhibitor and its potential ocular toxicity, the MSI technique is unmatched in its ability to predict drug toxicity in targeted organs [103].

MSI can demonstrate the rationality of chemical modifications, dosage form design, and nanomaterial selection for NPs during drug development

The targeting properties can be effectively improved through chemical modification, formulation optimization, or suitable nanomaterial selection for carriers. Based on its ability to display the compounds' spatial distribution, MSI can intuitively visualize the distribution of drugs after modifying their targeting properties, thus providing direct and unparalleled evidence and advantages for drug-targeting optimization studies. For example, to compare the in vivo distribution of paclitaxel injection, paclitaxel liposomes, and paclitaxel prodrugs, the air flow-assisted desorption electrospray ionization (AFADESI) Q-Orbitrap MSI instrument was used in this study to analyze the drug distributions in whole-body mouse sections at a spatial resolution of 350 μm . The results showed that paclitaxel injection and liposomes were widely distributed in multiple organs in the entire body after administration, with paclitaxel liposomes retained in vivo for a longer time compared with the paclitaxel injection. In comparison, the paclitaxel prodrug had good enrichment in targeted tumor tissues and was rarely detected in other organs or tissues [65] (Fig. 4d). Another exciting application of MSI techniques is in nanomedicine design. Tumor tissues have a lower pH in their tumor microenvironment when the c-Myc oncogene is highly expressed, while those with negative c-Myc expression have a relatively higher pH. pH-sensitive nanomedicines have been designed to target unique distributions based on pH differences in tumor tissues, and fast releasing (FR) and slow releasing (SR) nanomedicines have been designed based on the pH environment. The MALDI-TOF MSI platform at a spatial resolution of 50 μm was used to visualize the higher release and distribution of FR nanomedicines, which are formed by lipid chains, in low-pH tumor tissues in human subcutaneous tongue cancer with high c-Myc expression. In contrast, SR nanomedicines had a lower distribution in the same low-pH tumor environment (Fig. 4e). When evaluating these nanomedicines in human pancreatic cancer tumor tissues with low c-Myc expression, SR nanomedicines formed by aromatic ring chains presented a higher distribution in low c-Myc tumors than the FR nanomedicines. In the same study, the targeting properties of FR and SR nanomedicines were also visualized using the MALDI-TOF technique at the organ level. The results showed that FR and SR nanomedicines have a lower distribution in the liver and kidneys than in tumor tissues, indicating that the nanomedicines were successfully designed and modified to achieve a good targeting capability at the c-Myc expression level in tumor tissues [96].

In addition, nanomaterials play an increasingly important role in developing drug formulations. Their in vivo distribution properties have been highlighted and received increasing recognition. One exceptional property of nanomaterials is that they have innate characteristic MS signals under laser-based MSI platforms, such as MALDI, making it straightforward to track and analyze their spatial and temporal distributions [29, 104].

Currently, most MSI studies on the in vivo distribution of NPs have focused on a single compound, while few studies have analyzed the distribution of natural extracts in vivo using MSI techniques [105]. The main reason is the existence of isomers in the plant extracts. Due to the lack of a separation unit in the MSI instrument, it is challenging to distinguish ions of the same mass and identify the parent compounds from which the ions fragment. At the same time, many low-abundance compounds are present in the plant extract, which also increases the difficulty of deciphering the MSI data and their biological significance.

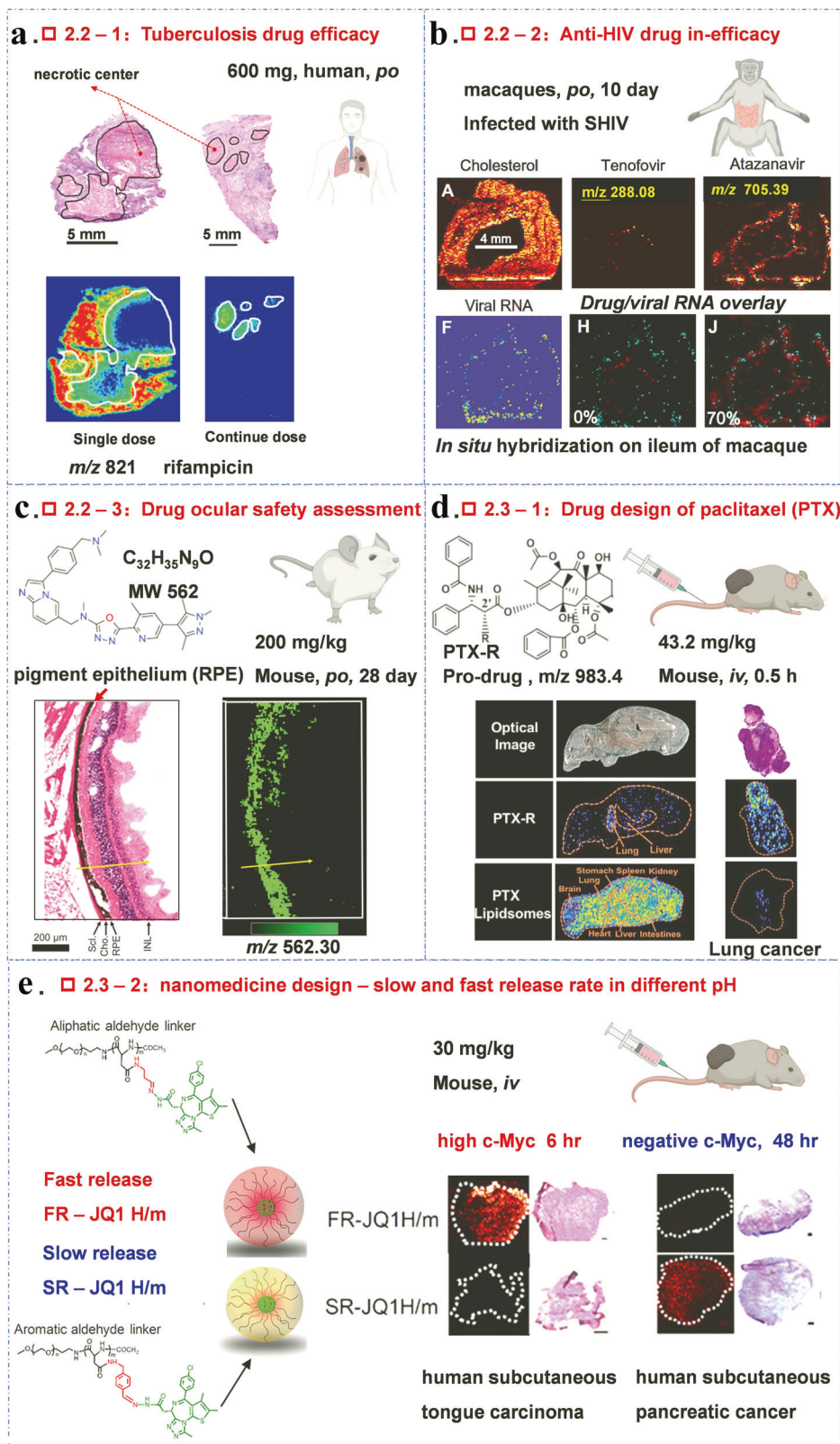


Fig. 4 Application of mass spectrometry imaging in accuracy and predictability of drugs efficacy & toxicity analysis and chemical modification & dosage forms design. **a** MALDI-LTQ XL-Orbitrap MSI spatial distribution of anti-tuberculosis drugs in the lung necrotic foci of human [98], with permission from Springer Nature. **b** IR-MALDI-Q-Orbitrap MSI spatial distribution of antiretroviral drugs in the ileum of macaques with SHIV [102], under the terms of the Creative Commons CC BY license. **c** MLADI-TOF MSI spatial distribution of MERTK inhibitor enriched in the retinal pigmented epithelium of mouse [104], under the terms of the Creative Commons CC BY license. **d** AFADESI-Q-Orbitrap MSI spatial distribution of paclitaxel lipidsomes and its pro-drug in the xenograft tumor mouse model [65], under the terms of the Creative Commons CC BY license. **e** MALDI-TOF MSI spatial distribution of two different release rate nanomedicines (slow and fast in different pH) in two tumors with different expression of c-Myc [97], with permission from American Chemical Society.

Considering the above problems, we propose four strategies that may improve the workflow of NP drug R&D. First, adopting MSI instruments coupled with high-resolution ion mobility features may be advantageous when studying the *in vivo* chemical distribution of extracts. The second is to develop *in situ* ion sources that are based on droplet microextraction combined with online nano separation, although one possible downside is that this strategy will significantly increase the complexity and analysis time of MSI data processing. The third strategy is to combine the classic LC-MS and MSI techniques to analyze small tissue samples on the square micron scale, where the compounds are also enriched. Finally, an indirect approach may be adopted by analyzing endogenous metabolites with the MSI technique, which may reflect the *in vivo* distribution and pharmacological characteristics of the plant extracts, especially for TCM [106].

CONSIDERATIONS FOR PERFORMING BETTER MSI STUDIES

The MSI technique provides a novel tool with a spatial perspective for new drug R&D from NPs. The following issues should be seriously considered or carefully optimized to obtain the desired MSI results.

Investigation modes influence the selection and optimization strategies of MSI

As an omics technique, investigation modes of MSI could be divided into a discovery-driven mode (similar to the untargeted approach) and validation-driven mode (similar to the targeted approach). In the discovery-driven mode, proposing a novel scientific hypothesis is the primary goal, which is attained by exploring the unknown spatial distribution of elements [107], small molecules [92], lipids [60], peptides [108], proteins [109] or N-glycans [110]. Then, other analytical or biological techniques will be applied in the following study to validate the hypothesis and elucidate the underlying mechanisms. For this mode, investigators should understand that the visualized results might be inconsistent with the truth, which means that different sample preparations, ion sources, and mass spectrometry instruments could affect the spatial distribution characteristics and species of molecular components. For the validation-driven mode, displaying the spatial distribution of target analytes is the primary experimental purpose. The MSI technique serves as a tool to directly visualize the previously unseen spatial distribution of target analytes and provide useful information for analyte research in combination with other analytical methods. Under this mode, the method of sample preparation, the parameters of the ion source, and the choice of mass spectrometry instrument should be reasonably selected or optimized based on the properties of the target analytes so that the best imaging sensitivity and spatial resolution can be obtained. In addition, the matrix effect *in situ* should also be considered when performing quantitative distribution analyses [32].

Sample preparation is a crucial step in the MSI workflow

The importance of sample handling has been repeatedly mentioned in several keynote MSI reviews [14, 18, 24, 111], some of which are specifically dedicated to this stage in the MSI workflow. Generally, the following five aspects should be considered during the MSI sample preparation stage: the selection of sample tissue types, tissue section acquisition methods, section processing methods, the choice of derivatization methods (if needed) [112, 113], and matrix selection and spray methods when using certain ion sources that require matrix assistance [112, 114].

Selection of sample tissue type. As mentioned above, various types of biological samples have been applied for MSI data acquisition, including plant tissues, snap-frozen animal and clinical tissues, and formalin-fixed paraffin-embedded (FFPE) tissues that

are commonly seen in clinical studies. Different sample types require different preparation methods and sometimes even novel methods to accommodate the particular properties of the sample [60]. The MSI technique can use fresh [52] or dry plant specimens [115], although the dried plant sample would be much more challenging [115]. Animal and clinical frozen tissues represent typical sample types that are applied and analyzed using the MSI technique. The tissue sample size can be small at the square millimeter level, such as the mouse retina [116], or on a relatively large scale, such as whole-body sections of adult rats [63]. In addition, the fresh bone tissues of mice could also be analyzed by MSI [117]. FFPE is the most abundant sample type preserved for clinical study and diagnosis [118]. Although some chemical components are denatured and lost during the treatment process, such as predehydration, the retained analytes can still provide valuable information regarding their spatial distribution to understand the underlying pathological mechanisms. The method of sample preparation for FFPE is much different from that of other samples [118].

Tissue section acquisition methods. The section preparation of plant samples is the most challenging. Due to the variety of plant sample types, the imprinting method is often used for fresh flowers and leaves in addition to the typical frozen sections. A more detailed comparison and summary of plant sample preparation methods can be found in a previous review [14]. Of note, when the plant samples are rich in oil [60], wax [52], starch, moisture, and fibers, the difficulty of preparing sample sections will be greatly increased, and the preparation step may even become the limiting step during MSI studies. Our laboratory proposed the use of a commercialized adhesive marketed for everyday household use to fix the oil-rich seed kernel and nut slice sections onto glass slides, which improved the spray pressure tolerance of the DESI ion source and successfully achieved spatial lipidomic analysis of these seed tissues [60]. One study on the whole plant developed a bidimensional (2D)-unidimensional (1D)-2D imprinting strategy with a string plane to overcome the limits of imaging large fresh plant samples [119]. For animal and clinical frozen tissue samples, frozen sections are generally obtained using a cryostat at a thickness of approximately 8–15 μm . Studies using FFPE tissue sections have reported that thin slices (approximately 1 μm) would be beneficial for improving the sensitivity of MSI detection [118, 120]. For whole-body sections containing bone tissues, a tungsten steel knife with higher hardness is usually required with a modified cryostat holder or a specialized cryomicrotome [121]. Generally, the tissue sections are transferred to regular glass slides for MSI application. For some special ion sources, such as MALDI, conductive indium tin oxide (ITO) slides are needed. Precoating ITO slides with gelatin and chromium potassium sulfate dodecahydrate would improve the adherence of FFPE sections, especially when the sections contain cartilage-bone, teeth, and mouse whole-body sections [122]. Specialized adhesive tapes could be used for mounting large tissue sections [63]. It is worth mentioning that the optimum cutting temperature (OCT) polymer, commonly used for frozen tissue embedding for immunohistochemistry (IHC) and immunofluorescence techniques, will produce a severe degree of ion suppression, which makes subsequent MSI data acquisition impossible [14]. Therefore, other embedding reagents, such as gelatin [123] and 2%–8% carboxymethyl cellulose (CMC) or their mixture, are recommended as alternative embedding media for MSI studies [121].

Section processing methods. After tissue sections are prepared, they are generally kept frozen and stored at ultralow temperature for long-term storage, and the slides are dried before use. Thus, the following three aspects can be optimized to obtain better MSI detection and data acquisition in this step. The first aspect is the

need to enhance or change the composition on the surface of the obtained tissue slices through section pretreatment. Except for SIMS and inductively coupled plasma–mass spectrometry (ICP–MS), whose ion sources are based on laser ablation technology (LD), the ion sources of the majority of MSI instruments are based on surface ionization technology [13]. This means that the components of the tissue surface on the slide would determine the analytes that the investigators will obtain in the MSI data. Therefore, with proper surface pretreatments, it is possible to alter the chemical composition of the tissue surface by removing the superficial wax or extracting the intracellular components from the tissue surface. For example, organic solvent treatment can remove the wax on some plant tissue surfaces [52], and organic solvent leaching can be applied to remove the paraffin on FFPE sections [118]. Additionally, using an in situ hydrogel conditioning method, the sensitivity of chemical components can be enhanced by as much as 2- to 25-fold in MSI [124]. When analyzing protein components, surface digestion with trypsin is commonly applied on the section surface, followed by in situ enzymatic peptide imaging and identification [125]. For N-glycan analysis, N-glycosidase F (PNGase F) is typically used for pretreatment to release the N-glycans bound to proteins for MSI analysis [126–128]. The second aspect is the need to enhance the accuracy in mass calibration [129] or quantification by introducing internal standards on the tissue surface before MSI acquisition [28, 64, 73, 78]. One study compared three methods of introducing internal standards onto the sample sections using DESI. The results showed that spraying the internal standard onto the tissue surface using specialized spraying equipment resulted in the best quantitative correction for the biological samples [130]. The third aspect includes the application of tissue pretreatments for stabilization and sterility purposes when working with potentially biohazard samples. Most MSI data acquisition steps take hours to complete and are performed at room temperature. It should be taken into consideration that the components on sample surfaces might change with time. In addition, some clinical samples may contain potentially infectious pathogens, such as bacteria and viruses; thus, proper pretreatments are required for pathogen inactivation or toxicant removal to ensure biosafety throughout the workflow [100, 131, 132].

Sample derivatization. Sample derivatization has two purposes: to enhance the ionization efficiency of difficult-to-ionize compounds [108, 133–139] and to increase the differentiation of isomers, such as lipid isomers with C=C double-bond (DB)

positions [140–145]. For the former purpose, some types of analytes, such as catecholamines [133], metabolism of sulfur-containing metabolites and proteins [135], neurotransmitters containing primary and secondary amines and phenolic hydroxyls [134, 138], cholesterol [137], and corticosteroids [139], have been derived with special chemical reagents to increase their ionization and sensitivity in MSI detection. In addition, identifying double bond isomerization of phospho- and glycolipids has always been the focus of spatial lipidomics. Some chemical reagents or methods, such as benzaldehyde [140] and benzophenone [143] or ozone-induced dissociation reactions [142], have been used to differentiate the lipid isomers with C=C double bonds. Several reviews on the sample derivatization strategies in MSI can be retrieved [112, 113, 146].

Matrix selection and spraying strategies. For the mainstream ion source represented by MALDI, a special organic acid must be introduced on the surface of the section before MALDI-MSI acquisition. It could take part in the ionization process by converting laser (UV 337 nm or 355 nm) energy into thermal energy to achieve molecular ionization of the substances in the matrix [14]. Therefore, the matrix would influence four aspects of MALDI-MSI: the analytes of a section should first be extracted into the matrix or the sensitivity may be too low; the size of the matrix crystal should be small enough to obtain high spatial resolution; the purity of the matrix should be high enough to reduce the background of MSI; and the thickness of the matrix layer on tissue sections should be as uniform as possible to obtain consistent responses and signals for MSI. More information related to MALDI matrices can be found in previous reviews [112, 114, 147]. On the other hand, the introduction of nanomaterials has led to the establishment of SALDI-MSI from MALDI-MSI, which is also covered in previous reviews [148, 149]. Of note, introducing matrix and derivatization reagents, including pretreatment with solvents, may cause the displacement of small molecules on the tissue surface. Therefore, it is necessary to investigate the effects of these pretreatments, especially for MSI analysis with a high spatial resolution (< 10 μm) [14].

Ion source selection plays a central role in the MSI workflow. The core component of the MSI instrument is the in situ ion source. Currently, based on the principle of on-tissue extraction and ionization, ion sources can be divided into three major categories (Table 2): laser- (UV or IR), liquid-, and ion cluster-based ion sources. The laser-based ion source, represented by MALDI, is

Table 2. Overview of ion sources used for MSI analysis [33, 42, 60, 80, 103, 149–158, 163–182].

Ion Source	Pressure	Matrix	Spatial resolution	Molecular range
• Laser based				
1. MALDI	Vacuum	Yes / Nano-materials	>5 μm	Small, large molecular
2. MALDI 2	Vacuum	Yes / Nano-materials	>1 μm	Small, large molecular
3. AP-MALDI	AP	Yes / Nano-materials	>1 μm	Preferred small molecular
4. SALDI	Vacuum	Nano-materials	>5 μm	Preferred small molecular
5. IR-MALDESI	AP	No / Yes	>50 μm	Preferred small molecular
• Liquid based				
6. DESI	AP	No	>50 μm	Preferred small molecular
7. AFA-DESI	AP	No	>100 μm	Preferred small molecular
8. nano-DESI	AP	No	>10 μm	Preferred small molecular
9. LESA	AP	No	>400 μm	Small, large molecular
• Ion cluster based				
10. SIMS	High vacuum	No	>50 nm	Preferred element, small molecular
11. nano-SIMS	High vacuum	No	>50 nm	Preferred element, small molecular

the most popular MSI instrument source at present, and more than 50% of MSI research uses MALDI, which is an MSI method with the broadest coverage of analytes and the most complicated analytical parameters [42]. Other MSIs with laser-based ion sources include MALDI2 [150–152], AP-MALDI [80, 153, 154], SALDI [148, 149, 155–157], and IR-MALDESI [158–161]. The liquid-based ion sources of MSIs are represented by DESI [33, 60, 102], which is also a rapidly expanding technique in terms of applications, and it presents the advantages of being matrix-free and having a simple analysis workflow. Other similar MSI techniques with liquid-based ion sources are AFADESI [162–165], nano-DESI [166–170], and liquid extraction surface analysis (LESA) [171–176]. The ion cluster-based ion sources are represented by SIMS [177–179] and nano-SIMS [180, 181], which higher equipment and working environment requirements than the other ion sources. The sample analysis is performed under high vacuum conditions, and the instruments are relatively large and expensive. However, SIMS provides unparalleled advantages in achieving single-cell or even subcellular resolution levels [177, 179, 181]. The above ion sources hold differences and preferences in the range of analytical molecules, spatial resolution, and sensitivity (Table 2). Therefore, the choice should be made based on the hypothesis and purpose of the study.

Impact of mass spectrometry instruments on MSI analysis cannot be ignored

Currently, common MS instruments coupled with in situ ion sources include QQQ [182], TOF [133, 183] or TOF-TOF MS [184–186], Q-TOF MS [52, 60], IT-TOF MS [187], Orbitrap series MS [47, 150], FT-ICR MS [76, 188, 189], and ICP-MS [190, 191]. ICP-MS is mainly used for element analysis, while other mass spectrometry instruments significantly differ in the mass analysis range, sensitivity, and mass resolution. For example, TOF-TOF MS performs well when analyzing molecules with high molecular weight (10 kDa and more). Q-TOF MS has certain mass discrimination, which is significantly affected by its parameter settings in the lower and higher molecular weight ranges. However, Q-TOF MS has good performance in obtaining MS/MS ion fragments. Orbitrap and FT-ICR have significant advantages in acquiring ultrahigh-resolution data, which is conducive to resolving complex MS signals. Their resolution can reach greater than $1 \times 10^5 \sim 3 \times 10^5$ (400 Da) [188, 192], even above 1×10^6 [189], whereas the common resolution of high-resolution MS is only $1 \times 10^4 \sim 3 \times 10^4$ (400 Da). Additionally, it has better sensitivity for analyzing small molecules. The relative disadvantage of FT-ICR is the high cost and longer analysis time in the ultrahigh resolution mode.

Ion mobility provides an isolation dimension to MSI

The principle of MSI is that the analytes are directly ionized and the ions enter the MS unit of the instrument without chromatographic separation, which significantly increases the complexity of MS analysis. Meanwhile, as the spatial resolution increases, the area covered by a single pixel approaches $100 \mu\text{m}^2$ on the biological samples, which is consistent with the single-cell level, thus posing a significant challenge to the analytical sensitivity. Ion mobility analysis can be achieved in an MS instrument [193]. After the ions enter the MS detector, ion separation at the millisecond level based on molecular shape, which is called collision cross-section (CCS), is performed before entering the mass analyzer (TOF or Orbitrap) at the microsecond level based on the m/z value [194]. There is a certain degree of orthogonality between the CCS and m/z of the ions. Therefore, the application of ion mobility in MSIs could increase the possibility of differentiating isomers with the same m/z values. Meanwhile, the CCS value is unique to ions and can be used to identify ions based on the m/z and MS/MS spectra. Several databases have supported m/z values in combination with CCS values for joint ion retrieval and

identification, such as The Human Metabolome Database (HMDB, <https://hmdb.ca/>), AllCCS (<http://allccs.zhulab.cn/>), and LIPID MAPS (<https://lipidmaps.org/>). It should be mentioned that the in situ MS/MS spectrum is difficult to obtain for MSI experiments due to the low sensitivity and complicated ion signals, especially for ions with low abundance in MSI data. Therefore, CCS values could enhance the identification efficiency of low-abundance ions [60]. In addition, ion mobility analysis is coupled with an ion enrichment process; thus, it increases the ion detection sensitivity by a factor of 2~10 [195]. Many MSI studies have adopted ion mobility [60, 93, 151, 168, 196–198]. One problem is that the resolution of ion mobility can only reach 40~60 (CCS/ Δ CCS) [193]. Currently, the application of cyclic ion mobility technology has greatly improved the separation performance of ion mobility, for which the resolution could reach 400 (CCS/ Δ CCS) [199] and would provide significantly improved performance and application for MSI technology.

Balance should be maintained among spatial resolution, mass resolution, sensitivity, and data acquisition time

For a $1 \text{ cm} \times 1 \text{ cm}$ tissue section, the MSI data acquisition time is approximately 2.8 h when the spatial resolution is set at $100 \mu\text{m} \times 100 \mu\text{m}$ (a total of 10^4 pixels are obtained in that area) and the mass spectrum acquisition speed per pixel is set at one second. If the spatial resolution is further reduced to $10 \mu\text{m} \times 10 \mu\text{m}$ at the single-cell level, 10^6 pixels will be collected in that area and the data acquisition time will reach 278 h, which is impossible to achieve. At this point, it is necessary to sacrifice MS resolution and sensitivity to achieve a higher acquisition speed. By reducing the acquisition time to 0.1 s, the overall data acquisition time can be reduced to 28 h. Increasing the acquisition time of individual pixels is conducive to enhancing the MSI sensitivity but also significantly prolongs the data acquisition time. A longer data acquisition time is expected for MSI instruments with higher MS resolution or high-performance ion mobility separation. High spatial resolution is conducive to improving the MSI image quality but also leads to an exponential increase in data capacity and acquisition time. Therefore, for different analytical purposes, such as large samples or studies requiring single-cell resolution, a reasonable spatial resolution should be chosen to balance mass spectrometry resolution, sensitivity, and acquisition time. The four factors (spatial resolution, mass resolution, sensitivity, and data acquisition time) are also the limitations of MSI which are still difficult to meet the needs of biologists. Further method development or even creative instrument should be proposed constantly. Especially for spatial resolution and sensitivity, it is preferred for single-cell and even subcellular levels spatial resolution with high sensitivity.

CONCLUSIONS AND PERSPECTIVE

MSI, as a fascinating visualization and analytical technique, has a unique role in new drug research and development from NPs. It can discover novel chemical structures of NPs in situ, explore new targeting organs of a candidate drug, guide the preparation design of drugs, and reveal the new mechanisms of a drug by providing high spatial resolution in situ information about thousands of molecules on a label-free basis. With the development of MSI technology, exciting and innovative applications in NP R&D are expected in the following four emerging aspects. First, the advances and improvements in spatial resolution and data acquisition speed would increase the likelihood of displaying and analyzing molecules at the single-cell and even subcellular levels. Thus, integrating MSI with existing cellular and molecular imaging techniques will provide more powerful methods of discovering and interpreting drug mechanisms. Second, the development of other spatial omics technologies, especially with the improvement of spatial transcriptomics at the single-cell resolution, will provide

a more robust analytical approach for studying spatiotemporal changes in drug efficacy. Third, further integration with ultrahigh resolution MSI and metabolic flux techniques will assist in better understanding the dynamic metabolic changes in the spatial dimensions of the tumor or disease microenvironment. Fourth, the establishment of public repositories and databases for published and sharable MSI data and the application of data mining tools/software will grant easy access to MSI techniques and promote the broader application of MSI.

In summary, the advancement of MSI in terms of the above four aspects will lead to the development of a powerful spatiotemporal analysis tool for better new drug R&D from NPs. However, as an invasive analytical technique, MSI must be performed using biological tissue sections, thus preventing it from revealing the dynamic distribution of molecules in living organisms in real time. The goal to achieving the real-time visualization and analysis of all molecules inside plants and animals represents a dream to be fulfilled and the primary driving force underlying technological advancement.

ACKNOWLEDGEMENTS

This study was supported by the grants from the STS (the Science and Technology Service Network Initiative of the Chinese Academy of Sciences) program (KFJ-STQYD-2021-03-003), and the National Natural Science Foundation of China (81530095, 81673591, 81973455, 81973470, 82003939, 82003915), National Key Research and Development Program of China (2018YFC1707900, 2018YFC1707001). Part of figures were created with BioRender.com.

ADDITIONAL INFORMATION

Competing interests: The authors declare no competing interests.

REFERENCES

- Newman DJ, Cragg GM. Natural products as sources of new drugs over the nearly four decades from 01/1981 to 09/2019. *J Nat Prod*. 2020;83:770–803.
- Zhu XZ, Li XY, Liu J. Recent pharmacological studies on natural products in China. *Eur J Pharmacol*. 2004;500:221–30.
- Wu WY, Hou JJ, Long HL, Yang WZ, Liang J, Guo DA. TCM-based new drug discovery and development in China. *Chin J Nat Med*. 2014;12:241–50.
- Li Y, Wu YL. How Chinese scientists discovered qinghaosu (artemisinin) and developed its derivatives? What are the future perspectives? *Med Trop (Mars)*. 1998;58:9–12.
- Wang R, Yan H, Tang XC. Progress in studies of huperzine A, a natural cholinesterase inhibitor from Chinese herbal medicine. *Acta Pharmacol Sin*. 2006;27:1–26.
- Wu WY, Wang YP. Pharmacological actions and therapeutic applications of *Salvia miltiorrhiza* depside salt and its active components. *Acta Pharmacol Sin*. 2012;33:1119–30.
- Atanasov AG, Zotchev SB, Dirsch VM, Supuran CT. Natural products in drug discovery: advances and opportunities. *Nat Rev Drug Discov*. 2021;20:200–16.
- Herter-Sprie GS, Kung AL, Wong KK. New cast for a new era: preclinical cancer drug development revisited. *J Clin Invest*. 2013;123:3639–45.
- Esquenazi E, Yang YL, Watrous J, Gerwick WH, Dorrestein PC. Imaging mass spectrometry of natural products. *Nat Prod Rep*. 2009;26:1521–34.
- de Jong M, Essers J, van Weerden WM. Imaging preclinical tumour models: improving translational power. *Nat Rev Cancer*. 2014;14:481–93.
- Kuzma BA, Pence IJ, Greenfield DA, Ho A, Evans CL. Visualizing and quantifying antimicrobial drug distribution in tissue. *Adv Drug Deliv Rev*. 2021;177:113942.
- Buchberger AR, DeLaney K, Johnson J, Li L. Mass Spectrometry Imaging: A Review of Emerging Advancements and Future Insights. *Anal Chem*. 2018;90:240–65.
- Spraker JE, Luu GT, Sanchez LM. Imaging mass spectrometry for natural products discovery: a review of ionization methods. *Nat Prod Rep*. 2020;37:150–62.
- Bjarnholt N, Li B, D'Alvise J, Janfelt C. Mass spectrometry imaging of plant metabolites—principles and possibilities. *Nat Prod Rep*. 2014;31:818–37.
- Shih CJ, Chen PY, Liaw CC, Lai YM, Yang YL. Bringing microbial interactions to light using imaging mass spectrometry. *Nat Prod Rep*. 2014;31:739–55.
- Jarmusch AK, Cooks RG. Emerging capabilities of mass spectrometry for natural products. *Nat Prod Rep*. 2014;31:730–8.
- Sumner LW, Lei Z, Nikolau BJ, Saito K. Modern plant metabolomics: advanced natural product gene discoveries, improved technologies, and future prospects. *Nat Prod Rep*. 2015;32:212–29.
- Dong Y, Li B, Aharoni A. More than pictures: when MS imaging meets histology. *Trends Plant Sci*. 2016;21:686–98.
- Peng L, Chen HG, Zhou X. Mass spectrometry imaging technology and its application in medicinal plants research. *Zhongguo Zhong Yao Za Zhi*. 2020;45:1023–33.
- Hu W, Han Y, Sheng Y, Wang Y, Pan Q, Nie H. Mass spectrometry imaging for direct visualization of components in plants tissues. *J Sep Sci*. 2021;44:3462–76.
- Kokesch-Himmelreich J, Wittek O, Race AM, Rakete S, Schlicht C, Busch U, et al. MALDI mass spectrometry imaging: From constituents in fresh food to ingredients, contaminants and additives in processed food. *Food Chem*. 2022;385:132529.
- Jiang H, Zhang Y, Liu Z, Wang X, He J, Jin H. Advanced applications of mass spectrometry imaging technology in quality control and safety assessments of traditional Chinese medicines. *J Ethnopharmacol*. 2022;284:114760.
- Ait-Belkacem R, Sellami L, Villard C, DePauw E, Calligaris D, Lafitte D. Mass spectrometry imaging is moving toward drug protein co-localization. *Trends Biotechnol*. 2012;30:466–74.
- Lietz CB, Gemperline E, Li L. Qualitative and quantitative mass spectrometry imaging of drugs and metabolites. *Adv Drug Deliv Rev*. 2013;65:1074–85.
- Prideaux B, Lenaerts A, Dartois V. Imaging and spatially resolved quantification of drug distribution in tissues by mass spectrometry. *Curr Opin Chem Biol*. 2018;44:93–100.
- Cologna SM. Mass Spectrometry Imaging of Cholesterol. *Adv Exp Med Biol*. 2019;1115:155–66.
- Jove M, Spencer J, Clench M, Loadman PM, Twelves C. Precision pharmacology: Mass spectrometry imaging and pharmacokinetic drug resistance. *Crit Rev Oncol Hematol*. 2019;141:153–62.
- Nishidate M, Hayashi M, Aikawa H, Tanaka K, Nakada N, Miura SI, et al. Applications of MALDI mass spectrometry imaging for pharmacokinetic studies during drug development. *Drug Metab Pharmacokinet*. 2019;34:209–16.
- de Maar JS, Sofias AM, Porta Siegel T, Vreeken RJ, Moonen C, Bos C, et al. Spatial heterogeneity of nanomedicine investigated by multiscale imaging of the drug, the nanoparticle and the tumour environment. *Theranostics*. 2020;10:1884–909.
- Grégoire S, Luengo GS, Hallegot P, Pena AM, Chen X, Bornschlöggl T, et al. Imaging and quantifying drug delivery in skin - Part 1: Autoradiography and mass spectrometry imaging. *Adv Drug Deliv Rev*. 2020;153:137–46.
- Wang T, Liu J, Luo X, Hu L, Lu H. Functional metabolomics innovates therapeutic discovery of traditional Chinese medicine derived functional compounds. *Pharmacol Ther*. 2021;224:107824.
- Unsihuay D, Mesa Sanchez D, Laskin J. Quantitative Mass Spectrometry Imaging of Biological Systems. *Annu Rev Phys Chem*. 2021;72:307–29.
- Soudah T, Zoabi A, Margulis K. Desorption electrospray ionization mass spectrometry imaging in discovery and development of novel therapies. *Mass Spectrom Rev*. 2021;1–28. <https://doi.org/10.1002/mas.21736>.
- Jiang H, Gao S, Hu G, He J, Jin H. Innovation in drug toxicology: Application of mass spectrometry imaging technology. *Toxicology*. 2021;464:153000.
- Mallah K, Zibara K, Kerbaj C, Eid A, Khoshman N, Ousseily Z et al. Neurotrauma investigation through spatial omics guided by mass spectrometry imaging: Target identification and clinical applications. *Mass Spectrom Rev*. 2021;1–17. <https://doi.org/10.1002/mas.21719>.
- Groessler M, Vogt B. Mass Spectrometry imaging and its place in nephrology. *Nephrol Dial Transpl*. 2021;gfab359. <https://doi.org/10.1093/ndt/gfab359>.
- Davoli E, Zucchetti M, Matteo C, Ubezio P, D'Incalci M, Morosi L. The space dimension at the micro level: mass spectrometry imaging of drugs in tissues. *Mass Spectrom Rev*. 2021;40:201–14.
- Bertzbach LD, Kaufer BB, Karger A. Applications of mass spectrometry imaging in virus research. *Adv Virus Res*. 2021;109:31–62.
- Ajith A, Sthanikam Y, Banerjee S. Chemical analysis of the human brain by imaging mass spectrometry. *Analyst*. 2021;146:5451–73.
- Santilli AML, Ren K, Oleschuk R, Kaufmann M, Rudan J, Fichtinger G, et al. Application of intraoperative mass spectrometry and data analytics for oncological margin detection, a review. *IEEE Trans Biomed Eng*. 2022; Pp.
- Zhao C, Cai Z. Three-dimensional quantitative mass spectrometry imaging in complex system: From subcellular to whole organism. *Mass Spectrom Rev*. 2022;41:469–87.
- Baker TC, Han J, Borchers CH. Recent advancements in matrix-assisted laser desorption/ionization mass spectrometry imaging. *Curr Opin Biotechnol*. 2017;43:62–9.
- He C, Fong LG, Young SG, Jiang H. NanoSIMS imaging: an approach for visualizing and quantifying lipids in cells and tissues. *J Investig Med*. 2017;65:669–72.

44. Noun M, Akoume R, Abbas I. Cell and Tissue Imaging by TOF-SIMS and MALDI-TOF: an overview for biological and pharmaceutical analysis. *Microsc Microanal*. 2021;28:1–26.
45. Heskes AM, Sundram TCM, Boughton BA, Jensen NB, Hansen NL, Crocoll C, et al. Biosynthesis of bioactive diterpenoids in the medicinal plant *Vitex agnus-castus*. *Plant J*. 2018;93:943–58.
46. Li B, Neumann EK, Ge J, Gao W, Yang H, Li P, et al. Interrogation of spatial metabolome of *Ginkgo biloba* with high-resolution matrix-assisted laser desorption/ionization and laser desorption/ionization mass spectrometry imaging. *Plant Cell Environ*. 2018;41:2693–703.
47. Tocci N, Gaid M, Kaftan F, Belkheir AK, Belhadj I, Liu B, et al. Exodermis and endodermis are the sites of xanthone biosynthesis in *Hypericum perforatum* roots. *N Phytol*. 2018;217:1099–112.
48. Kuo TH, Huang HC, Hsu CC. Mass spectrometry imaging guided molecular networking to expedite discovery and structural analysis of agarwood natural products. *Anal Chim Acta*. 2019;1080:95–103.
49. Francese S, Bradshaw R, Flinders B, Mitchell C, Bleay S, Cicero L, et al. Curcumin: a multipurpose matrix for MALDI mass spectrometry imaging applications. *Anal Chem*. 2013;85:5240–8.
50. Yamamoto K, Takahashi K, Caputi L, Mizuno H, Rodriguez-Lopez CE, Iwasaki T, et al. The complexity of intercellular localisation of alkaloids revealed by single-cell metabolomics. *N Phytol*. 2019;224:848–59.
51. Sun C, Liu W, Ma S, Zhang M, Geng Y, Wang X. Development of a high-coverage matrix-assisted laser desorption/ionization mass spectrometry imaging method for visualizing the spatial dynamics of functional metabolites in *Salvia miltiorrhiza* Bge. *J Chromatogr A*. 2020;1614:460704.
52. Tong Q, Zhang C, Tu Y, Chen J, Li Q, Zeng Z, et al. Biosynthesis-based spatial metabolome of *Salvia miltiorrhiza* Bunge by combining metabolomics approaches with mass spectrometry-imaging. *Talanta*. 2022;238:123045.
53. Conceição RS, Perez CJ, Branco A, Botura MB, Iffa DR. Identification of Sassafras alkaloids by high-performance thin-layer chromatography tandem mass spectrometry and mapping by desorption electrospray ionization mass spectrometry imaging. *J Mass Spectrom*. 2021;56:e4674.
54. Li B, Ge J, Liu W, Hu D, Li P. Unveiling spatial metabolome of *Paeonia suffruticosa* and *Paeonia lactiflora* roots using MALDI MS imaging. *N Phytol*. 2021;231:892–902.
55. Sun C, Ma S, Li L, Wang D, Liu W, Liu F, et al. Visualizing the distributions and spatiotemporal changes of metabolites in *Panax notoginseng* by MALDI mass spectrometry imaging. *J Ginseng Res*. 2021;45:726–33.
56. Tang X, Zhao M, Chen Z, Huang J, Chen Y, Wang F, et al. Visualizing the spatial distribution of metabolites in *Clausena lansium* (Lour.) Skeels using matrix-assisted laser desorption/ionization mass spectrometry imaging. *Phytochemistry*. 2021;192:112930.
57. Yang Y, Yang Y, Qiu H, Ju Z, Shi Y, Wang Z, et al. Localization of constituents for determining the age and parts of ginseng through ultraperformance liquid chromatography quadrupole/time of flight-mass spectrometry combined with desorption electrospray ionization mass spectrometry imaging. *J Pharm Biomed Anal*. 2021;193:113722.
58. Zhao WH, Zhang YD, Shi YP. Visualizing the spatial distribution of endogenous molecules in wolfberry fruit at different development stages by matrix-assisted laser desorption/ionization mass spectrometry imaging. *Talanta*. 2021;234:122687.
59. Zhao Y, Chu S, Gui S, Qin Y, Xu R, Shan T, et al. Tissue-specific metabolite profiling of *Fallopia multiflora* (Heshouwu) and *Fallopia multiflora* var. *angulata* by mass spectrometry imaging and laser microdissection combined with UPLC-Q/TOF-MS. *J Pharm Biomed Anal*. 2021;200:114070.
60. Hou J, Zhang Z, Zhang L, Wu W, Huang Y, Jia Z, et al. Spatial lipidomics of eight edible nuts by desorption electrospray ionization with ion mobility mass spectrometry imaging. *Food Chem*. 2022;371:130893.
61. Zhang C, Žukauskaitė A, Petřík I, Pěncík A, Hönl M, Grúz J, et al. In situ characterisation of phytohormones from wounded *Arabidopsis* leaves using desorption electrospray ionisation mass spectrometry imaging. *Analyst*. 2021;146:2653–63.
62. Rodrigues JP, Prova SS, Moraes LAB, Iffa DR. Characterization and mapping of secondary metabolites of *Streptomyces* sp. from caatinga by desorption electrospray ionization mass spectrometry (DESI-MS). *Anal Bioanal Chem*. 2018;410:7135–44.
63. Luo Z, Liu D, Pang X, Yang W, He J, Zhang R, et al. Whole-body spatially-resolved metabolomics method for profiling the metabolic differences of epimer drug candidates using ambient mass spectrometry imaging. *Talanta*. 2019;202:198–206.
64. Tang W, Chen J, Zhou J, Ge J, Zhang Y, Li P, et al. Quantitative MALDI imaging of spatial distributions and dynamic changes of tetrandrine in multiple organs of rats. *Theranostics*. 2019;9:932–44.
65. Zhang J, Du Q, Song X, Gao S, Pang X, Li Y, et al. Evaluation of the tumor-targeting efficiency and intratumor heterogeneity of anticancer drugs using quantitative mass spectrometry imaging. *Theranostics*. 2020;10:2621–30.
66. Matsumoto T, Ikarashi Y, Takiyama M, Watanabe J, Setou M. Brain distribution of geissoschizine methyl ether in rats using mass spectrometry imaging analysis. *Sci Rep*. 2020;10:7293.
67. Wang T, Lee HK, Yue GGL, Chung ACK, Lau CBS, Cai Z. A novel binary matrix consisting of graphene oxide and caffeic acid for the analysis of scutellarin and its metabolites in mouse kidney by MALDI imaging. *Analyst*. 2021;146:289–95.
68. Gao L, Zhang Z, Wu W, Deng Y, Zhi H, Long H, et al. Quantitative imaging of natural products in fine brain regions using desorption electrospray ionization mass spectrometry imaging (DESI-MSI): *Uncaria* alkaloids as a case study. *Anal Bioanal Chem*. 2022;414:4999–5007.
69. Hansen HT, Janfelt C. Aspects of quantitation in mass spectrometry imaging investigated on cryo-sections of spiked tissue homogenates. *Anal Chem*. 2016;88:11513–20.
70. Russo C, Brickelbank N, Duckett C, Mellor S, Rumbelow S, Clench MR. Quantitative investigation of terbinafine hydrochloride absorption into a living skin equivalent model by MALDI-MSI. *Anal Chem*. 2018;90:10031–8.
71. Rzagalinski I, Kovačević B, Hainz N, Meier C, Tschernig T, Volmer DA. Toward higher sensitivity in quantitative MALDI imaging mass spectrometry of CNS drugs using a nonpolar matrix. *Anal Chem*. 2018;90:12592–600.
72. Swales JG, Dexter A, Hamm G, Nilsson A, Strittmatter N, Michopoulos F, et al. Quantitation of endogenous metabolites in mouse tumors using mass-spectrometry imaging. *Anal Chem*. 2018;90:6051–8.
73. Källback P, Vallianatou T, Nilsson A, Shariatgorji R, Schintu N, Pereira M, et al. Cross-validated matrix-assisted laser desorption/ionization mass spectrometry imaging quantitation protocol for a pharmaceutical drug and its drug-target effects in the brain using time-of-flight and Fourier transform ion cyclotron resonance analyzers. *Anal Chem*. 2020;92:14676–84.
74. Wu Q, Rubakhin SS, Sweedler JV. Quantitative imprint mass spectrometry imaging of endogenous ceramides in rat brain tissue with kinetic calibration. *Anal Chem*. 2020;92:6613–21.
75. Luptáková D, Vallianatou T, Nilsson A, Shariatgorji R, Hammarlund-Udenaes M, Loryan I, et al. Neuropharmacokinetic visualization of regional and subregional unbound antipsychotic drug transport across the blood-brain barrier. *Mol Psychiatry*. 2021;26:7732–45.
76. Huizing LRS, McDuffie J, Cuyckens F, van Heerden M, Koudriakova T, Heeren RMA, et al. Quantitative mass spectrometry imaging to study drug distribution in the intestine following oral dosing. *Anal Chem*. 2021;93:2144–51.
77. Lee A, Wang N, Carter CL, Zimmerman M, Dartois V, Shaw KJ, et al. Therapeutic potential of fosmanogepix (apx001) for intra-abdominal candidiasis: from lesion penetration to efficacy in a mouse model. *Antimicrob Agents Chemother*. 2021;65:e02476–20.
78. Dewez F, De Pauw E, Heeren RMA, Balluff B. Multilabel per-pixel quantitation in mass spectrometry imaging. *Anal Chem*. 2021;93:1393–400.
79. Handler AM, Pommergaard Pedersen G, Troensegaard Nielsen K, Janfelt C, Just Pedersen A, Clench MR. Quantitative MALDI mass spectrometry imaging for exploring cutaneous drug delivery of tofacitinib in human skin. *Eur J Pharm Biopharm*. 2021;159:1–10.
80. Morosi L, Matteo C, Meroni M, Ceruti T, Fuso Nerini I, Bello E, et al. Quantitative measurement of pioglitazone in neoplastic and normal tissues by AP-MALDI mass spectrometry imaging. *Talanta*. 2022;237:122918.
81. Hahm TH, Matsui T, Tanaka M. Matrix-assisted laser desorption/ionization mass spectrometry imaging of tissues via the formation of reproducible matrix crystals by the fluorescence-assisted spraying method: a quantification approach. *Anal Chem*. 2022;94:1990–8.
82. Wu W, Hou J, Zhang Z, Li F, Zhang R, Gao L, et al. Information entropy-based strategy for the quantitative evaluation of extensive hyperspectral images to better unveil spatial heterogeneity in mass spectrometry imaging. *Anal Chem*. 2022;94:10355–66.
83. Eberlin LS, Mulcahy JV, Tzabazis A, Zhang J, Liu H, Logan MM, et al. Visualizing dermal permeation of sodium channel modulators by mass spectrometric imaging. *J Am Chem Soc*. 2014;136:6401–5.
84. Taudorf EH, Lerche CM, Vissing AC, Philipssen PA, Hannibal J, D'Alvise J, et al. Topically applied methotrexate is rapidly delivered into skin by fractional laser ablation. *Expert Opin Drug Deliv*. 2015;12:1059–69.
85. Wenande E, Olesen UH, Nielsen MM, Janfelt C, Hansen SH, Anderson RR, et al. Fractional laser-assisted topical delivery leads to enhanced, accelerated and deeper cutaneous 5-fluorouracil uptake. *Expert Opin Drug Deliv*. 2017;14:307–17.
86. Wang F, Yang P, Choi JS, Antovski P, Zhu Y, Xu X, et al. Cross-linked fluorescent supramolecular nanoparticles for intradermal controlled release of antifungal drug-A therapeutic approach for onychomycosis. *ACS Nano*. 2018;12:6851–9.
87. Hendel K, Hansen ACN, Bik L, Bagger C, van Doorn MBA, Janfelt C, et al. Bleomycin administered by laser-assisted drug delivery or intradermal needle-injection results in distinct biodistribution patterns in skin: in vivo investigations with mass spectrometry imaging. *Drug Deliv*. 2021;28:1141–9.

88. Thompson CG, Rosen EP, Prince HMA, White N, Sykes C, de la Cruz G, et al. Heterogeneous antiretroviral drug distribution and HIV/SHIV detection in the gut of three species. *Sci Transl Med.* 2019;11:eaa8758.
89. Vallianatou T, Strittmatter N, Nilsson A, Shariatgorji M, Hamm G, Pereira M, et al. A mass spectrometry imaging approach for investigating how drug-drug interactions influence drug blood-brain barrier permeability. *Neuroimage.* 2018;172:808–16.
90. Strittmatter N, Richards FM, Race AM, Ling S, Sutton D, Nilsson A, et al. Method to visualize the intratumor distribution and impact of gemcitabine in pancreatic ductal adenocarcinoma by multimodal imaging. *Anal Chem.* 2022;94:1795–803.
91. Muzzi M, Gerace E, Buonvicino D, Coppi E, Resta F, Formentini L, et al. Dextramipexole improves bioenergetics and outcome in experimental stroke. *Br J Pharmacol.* 2018;175:272–83.
92. Arai S, Takeuchi S, Fukuda K, Taniguchi H, Nishiyama A, Tanimoto A, et al. Aisimertinib overcomes alectinib resistance caused by amphiregulin in a leptomenigeal carcinomatosis model of ALK-rearranged lung cancer. *J Thorac Oncol.* 2020;15:752–65.
93. Pang X, Gao S, Ga M, Zhang J, Luo Z, Chen Y, et al. Mapping metabolic networks in the brain by ambient mass spectrometry imaging and metabolomics. *Anal Chem.* 2021;93:6746–54.
94. Guo R, Zhou L, Chen X. Desorption electrospray ionization (DESI) source coupling ion mobility mass spectrometry for imaging fluoropezil (DC20) distribution in rat brain. *Anal Bioanal Chem.* 2021;413:5835–47.
95. Prasad M, Postma G, Franceschi P, Morosi L, Giordano S, Falcetta F, et al. A methodological approach to correlate tumor heterogeneity with drug distribution profile in mass spectrometry imaging data. *Gigascience.* 2020;9:giaa131.
96. Wei D, Yu Y, Huang Y, Jiang Y, Zhao Y, Nie Z, et al. A near-infrared-II polymer with tandem fluorophores demonstrates superior biodegradability for simultaneous drug tracking and treatment efficacy feedback. *ACS Nano.* 2021;15:5428–38.
97. Shibasaki H, Kinoh H, Cabral H, Quader S, Mochida Y, Liu X, et al. Efficacy of pH-sensitive nanomedicines in tumors with different c-MYC expression depends on the intratumoral activation profile. *ACS Nano.* 2021;15:5545–59.
98. Pridaux B, Via LE, Zimmerman MD, Eum S, Sarathy J, O'Brien P, et al. The association between sterilizing activity and drug distribution into tuberculosis lesions. *Nat Med.* 2015;21:1223–7.
99. Blanc L, Lenaerts A, Dartois V, Pridaux B. Visualization of mycobacterial biomarkers and tuberculosis drugs in infected tissue by MALDI-MS imaging. *Anal Chem.* 2018;90:6275–82.
100. Blanc L, Daudelin IB, Podell BK, Chen PY, Zimmerman M, Martinot AJ, et al. High-resolution mapping of fluoroquinolones in TB rabbit lesions reveals specific distribution in immune cell types. *Elife.* 2018;7:e41115.
101. Kokesch-Himmelreich J, Treu A, Race AM, Walter K, Hölscher C, Römpf A. Do anti-tuberculosis drugs reach their target?—high-resolution matrix-assisted laser desorption/ionization mass spectrometry imaging provides information on drug penetration into necrotic granulomas. *Anal Chem.* 2022;94:5483–92.
102. Rosen EP, Deleage C, White N, Sykes C, Brands C, Adamson L, et al. Antiretroviral drug exposure in lymph nodes is heterogeneous and drug dependent. *J Int AIDS Soc.* 2022;25:e25895.
103. Zhao X, Huang X, Zhang X, Shi J, Jia X, Zhu K, et al. Distribution visualization of the chlorinated disinfection byproduct of diazepam in zebrafish with desorption electrospray ionization mass spectrometry imaging. *Talanta.* 2022;237:122919.
104. Hamm G, Maglennon G, Williamson B, Macdonald R, Doherty A, Jones S, et al. Pharmacological inhibition of MERTK induces in vivo retinal degeneration: a multimodal imaging ocular safety assessment. *Arch Toxicol.* 2022;96:613–24.
105. Xue J, Liu H, Chen S, Xiong C, Zhan L, Sun J, et al. Mass spectrometry imaging of the in situ drug release from nanocarriers. *Sci Adv.* 2018;4:eaat9039.
106. Matsumoto T, Kushida H, Matsushita S, Oyama Y, Suda T, Watanabe J, et al. Distribution analysis via mass spectrometry imaging of ephedrine in the lungs of rats orally administered the Japanese Kampo Medicine Maoto. *Sci Rep.* 2017;7:44098.
107. Li Y, Wu Q, Hu E, Wang Y, Lu H. Quantitative mass spectrometry imaging of metabolomes and lipidomes for tracking changes and therapeutic response in traumatic brain injury surrounding injured area at chronic phase. *ACS Chem Neurosci.* 2021;12:1363–75.
108. Theiner S, Schweikert A, Van Malderen SJM, Schoeberl A, Neumayer S, Jilma P, et al. Laser ablation-inductively coupled plasma time-of-flight mass spectrometry imaging of trace elements at the single-cell level for clinical practice. *Anal Chem.* 2019;91:8207–12.
109. Li K, Guo S, Tang W, Li B. Characterizing the spatial distribution of dipeptides in rodent tissue using MALDI MS imaging with on-tissue derivatization. *Chem Commun (Camb).* 2021;57:12460–3.
110. Hale OJ, Hughes JW, Sisley EK, Cooper HJ. Native ambient mass spectrometry enables analysis of intact endogenous protein assemblies up to 145 kDa directly from tissue. *Anal Chem.* 2022;94:5608–14.
111. Ščupáková K, Adelaja OT, Balluff B, Ayyappan V, Tressler CM, Jenkinson NM, et al. Clinical importance of high-mannose, fucosylated, and complex N-glycans in breast cancer metastasis. *JCI Insight.* 2021;6:e146945.
112. Tuck M, Blanc L, Touti R, Patterson NH, Van Nuffel S, Villette S, et al. Multimodal imaging based on vibrational spectroscopies and mass spectrometry imaging applied to biological tissue: a multiscale and multiomics review. *Anal Chem.* 2021;93:445–77.
113. Zhou Q, Fülöp A, Hopf C. Recent developments of novel matrices and on-tissue chemical derivatization reagents for MALDI-MSI. *Anal Bioanal Chem.* 2021;413:2599–617.
114. Merdas M, Lagarrigue M, Vanbellingen Q, Umbdenstock T, Da Violante G, Pineau C. On-tissue chemical derivatization reagents for matrix-assisted laser desorption/ionization mass spectrometry imaging. *J Mass Spectrom.* 2021;56:e4731.
115. Borisov RS, Matveeva MD, Zaikin VG. Reactive matrices for analytical matrix-assisted laser desorption/ionization (MALDI) mass spectrometry. *Crit Rev Anal Chem.* 2021:1–17.
116. Shimma S, Sagawa T. Microscopy and mass spectrometry imaging reveals the distributions of curcumin species in dried turmeric root. *J Agric Food Chem.* 2019;67:9652–7.
117. Bonnin EA, Fornasiero EF, Lange F, Turck CW, Rizzoli SO. NanoSIMS observations of mouse retinal cells reveal strict metabolic controls on nitrogen turnover. *BMC Mol Cell Biol.* 2021;22:5.
118. Good CJ, Neumann EK, Butrico CE, Cassat JE, Caprioli RM, Spraggins JM. High spatial resolution MALDI imaging mass spectrometry of fresh-frozen bone. *Anal Chem.* 2022;94:3165–72.
119. Ly A, Buck A, Balluff B, Sun N, Gorzalka K, Feuchtinger A, et al. High-mass-resolution MALDI mass spectrometry imaging of metabolites from formalin-fixed paraffin-embedded tissue. *Nat Protoc.* 2016;11:1428–43.
120. Wang Y, Xia B, Deng S, Ye Y, Zhou Y. Performing 2D-1D-2D mass spectrometry imaging using strings. *Anal Chem.* 2022;94:1661–8.
121. Longuespée R, Kriegsmann K, Cremer M, Zgorzelski C, Casadonte R, Kazdal D, et al. In MALDI-mass spectrometry imaging on formalin-fixed paraffin-embedded tissue specimen section thickness significantly influences m/z peak intensity. *Proteom Clin Appl.* 2019;13:e1800074.
122. Vandenbosch M, Nauta SP, Svirikova A, Poeze M, Heeren RMA, Siegel TP, et al. Sample preparation of bone tissue for MALDI-MSI for forensic and (pre)clinical applications. *Anal Bioanal Chem.* 2021;413:2683–94.
123. Lee YR, Briggs MT, Kuliwaba JS, Anderson PH, Condina MR, Hoffmann P. Gelatin-coated indium tin oxide slides improve human cartilage-bone tissue adherence and N-glycan signal intensity for mass spectrometry imaging. *Anal Bioanal Chem.* 2021;413:2675–82.
124. Gill EL, Yost RA, Vedam-Mai V, Garrett TJ. Precast gelatin-based molds for tissue embedding compatible with mass spectrometry imaging. *Anal Chem.* 2017;89:576–80.
125. Song X, Luo Z, Li X, Li T, Wang Z, Sun C, et al. In situ hydrogel conditioning of tissue samples to enhance the drug's sensitivity in ambient mass spectrometry imaging. *Anal Chem.* 2017;89:6318–23.
126. Andrews WT, Bickner AN, Tobias F, Ryan KA, Bruening ML, Hummon AB. Electroblooming through enzymatic membranes to enhance molecular tissue imaging. *J Am Soc Mass Spectrom.* 2021;32:1689–99.
127. Heijs B, Potthoff A, Soltwisch J, Dreisewerd K. MALDI-2 for the enhanced analysis of N-linked glycans by mass spectrometry imaging. *Anal Chem.* 2020;92:13904–11.
128. West CA, Lu X, Grimsley G, Norris-Caneda K, Mehta AS, Angel PM, et al. Optimization of multiple glycosidase and chemical stabilization strategies for N-Glycan isomer detection by mass spectrometry imaging in formalin-fixed, paraffin-embedded tissues. *Methods Mol Biol.* 2021;2271:303–16.
129. Pace CL, Angel PM, Drake RR, Muddiman DC. Mass spectrometry imaging of N-linked glycans in a formalin-fixed paraffin-embedded human prostate by infrared matrix-assisted laser desorption electrospray ionization. *J Proteome Res.* 2022;21:243–9.
130. Treu A, Römpf A. Matrix ions as internal standard for high mass accuracy matrix-assisted laser desorption/ionization mass spectrometry imaging. *Rapid Commun Mass Spectrom.* 2021;35:e9110.
131. Perez CJ, Ifa DR. Internal standard application strategies in mass spectrometry imaging by desorption electrospray ionization mass spectrometry. *Rapid Commun Mass Spectrom.* 2021;35:e9053.
132. Wang N, Sarathy JP, Zimmerman M, Kaya F, Wang H, Dartois V, et al. On-slide heat sterilization enables mass spectrometry imaging of tissue infected with high-threat pathogens outside of biocontainment: a study directed at mycobacterium tuberculosis. *J Am Soc Mass Spectrom.* 2021;32:2664–74.

133. Dannhorn A, Ling S, Powell S, McCall E, Maglennon G, Jones GN, et al. Evaluation of UV-C decontamination of clinical tissue sections for spatially resolved analysis by mass spectrometry imaging (MSI). *Anal Chem.* 2021;93:2767–75.
134. Kaya I, Brülls SM, Dunevall J, Jennische E, Lange S, Mårtensson J, et al. On-tissue chemical derivatization of catecholamines using 4-(*n*-methyl)pyridinium boronic acid for ToF-SIMS and LDI-ToF mass spectrometry imaging. *Anal Chem.* 2018;90:13580–90.
135. Shariatgorji M, Nilsson A, Fridjonsdottir E, Vallianatou T, Källback P, Katan L, et al. Comprehensive mapping of neurotransmitter networks by MALDI-MS imaging. *Nat Methods.* 2019;16:1021–8.
136. Fülöp A, Bausbacher T, Rizzo S, Zhou Q, Gilland H, Hopf C, et al. New derivatization reagent for detection of free thiol-groups in metabolites and proteins in matrix-assisted laser desorption/ionization mass spectrometry imaging. *Anal Chem.* 2020;92:6224–8.
137. Sun C, Liu W, Geng Y, Wang X. On-tissue derivatization strategy for mass spectrometry imaging of carboxyl-containing metabolites in biological tissues. *Anal Chem.* 2020;92:12126–31.
138. Angelini R, Yutuc E, Wyatt MF, Newton J, Yusuf FA, Griffiths L, et al. Visualizing cholesterol in the brain by on-tissue derivatization and quantitative mass spectrometry imaging. *Anal Chem.* 2021;93:4932–43.
139. Shariatgorji R, Nilsson A, Fridjonsdottir E, Strittmatter N, Dannhorn A, Svenningsson P, et al. Spatial visualization of comprehensive brain neurotransmitter systems and neuroactive substances by selective *in situ* chemical derivatization mass spectrometry imaging. *Nat Protoc.* 2021;16:3298–321.
140. Zecchi R, Franceschi P, Tigli L, Amidani D, Catozzi C, Ricci F, et al. Sample preparation strategy for the detection of steroid-like compounds using MALDI mass spectrometry imaging: pulmonary distribution of budesonide as a case study. *Anal Bioanal Chem.* 2021;413:4363–71.
141. Bednařík A, Bölsker S, Soltwisch J, Dreisewerd K. An on-tissue paterno-büchi reaction for localization of carbon-carbon double bonds in phospholipids and glycolipids by matrix-assisted laser-desorption-ionization mass-spectrometry imaging. *Angew Chem Int Ed Engl.* 2018;57:12092–6.
142. Klein DR, Feider CL, Garza KY, Lin JQ, Eberlin LS, Brodbelt JS. Desorption electrospray ionization coupled with ultraviolet photodissociation for characterization of phospholipid isomers in tissue sections. *Anal Chem.* 2018;90:10100–4.
143. Paine MRL, Poad BLJ, Eijkel GB, Marshall DL, Blanksby SJ, Heeren RMA, et al. Mass spectrometry imaging with isomeric resolution enabled by ozone-induced dissociation. *Angew Chem Int Ed Engl.* 2018;57:10530–4.
144. Wäldchen F, Spengler B, Heiles S. Reactive matrix-assisted laser desorption/ionization mass spectrometry imaging using an intrinsically photoreactive paterno-büchi matrix for double-bond localization in isomeric phospholipids. *J Am Chem Soc.* 2019;141:11816–20.
145. Bednařík A, Preisler J, Bezdeková D, Macháľková M, Hendrych M, Navrátilová J, et al. Ozonization of tissue sections for MALDI MS imaging of carbon-carbon double bond positional isomers of phospholipids. *Anal Chem.* 2020;92:6245–50.
146. Zhang J, Huo X, Guo C, Ma X, Huang H, He J, et al. Rapid imaging of unsaturated lipids at an isomeric level achieved by controllable oxidation. *Anal Chem.* 2021;93:2114–24.
147. Harkin C, Smith KW, Cruickshank FL, Logan Mackay C, Flinders B, Heeren RMA, et al. On-tissue chemical derivatization in mass spectrometry imaging. *Mass Spectrom Rev.* 2021;41:662–94.
148. Schulz S, Becker M, Groseclose MR, Schadt S, Hopf C. Advanced MALDI mass spectrometry imaging in pharmaceutical research and drug development. *Curr Opin Biotechnol.* 2019;55:51–9.
149. Müller WH, De Pauw E, Far J, Malherbe C, Eppe G. Imaging lipids in biological samples with surface-assisted laser desorption/ionization mass spectrometry: A concise review of the last decade. *Prog Lipid Res.* 2021;83:101114.
150. Müller WH, Verdin A, De Pauw E, Malherbe C, Eppe G. Surface-assisted laser desorption/ionization mass spectrometry imaging: A review. *Mass Spectrom Rev.* 2022;41:373–420.
151. Niehaus M, Soltwisch J, Belov ME, Dreisewerd K. Transmission-mode MALDI-2 mass spectrometry imaging of cells and tissues at subcellular resolution. *Nat Methods.* 2019;16:925–31.
152. Soltwisch J, Heijs B, Koch A, Vens-Cappell S, Höhndorf J, Dreisewerd K. MALDI-2 on a trapped ion mobility quadrupole time-of-flight instrument for rapid mass spectrometry imaging and ion mobility separation of complex lipid profiles. *Anal Chem.* 2020;92:8697–703.
153. Bien T, Bessler S, Dreisewerd K, Soltwisch J. Transmission-mode MALDI mass spectrometry imaging of single cells: optimizing sample preparation protocols. *Anal Chem.* 2021;93:4513–20.
154. Kompauer M, Heiles S, Spengler B. Atmospheric pressure MALDI mass spectrometry imaging of tissues and cells at 1.4- μ m lateral resolution. *Nat Methods.* 2017;14:90–6.
155. Kompauer M, Heiles S, Spengler B. Autofocusing MALDI mass spectrometry imaging of tissue sections and 3D chemical topography of nonflat surfaces. *Nat Methods.* 2017;14:1156–8.
156. Iakab SA, Ráfols P, Tajés M, Correig-Blanchar X, García-Altres M. Gold nanoparticle-assisted black silicon substrates for mass spectrometry imaging applications. *ACS Nano.* 2020;14:6785–94.
157. Müller WH, Verdin A, Kune C, Far J, De Pauw E, Malherbe C, et al. Dual-polarity SALDI FT-ICR MS imaging and Kendrick mass defect data filtering for lipid analysis. *Anal Bioanal Chem.* 2021;413:2821–30.
158. Wang XN, Li B. Monolithic gold nanoparticles/Thiol- β -cyclodextrin-functionalized TiO₂(2) nanowires for enhanced SALDI MS detection and imaging of natural products. *Anal Chem.* 2022;94:952–9.
159. Bokhart MT, Manni J, Garrard KP, Ekelöf M, Nazari M, Muddiman DC. IR-MALDESI mass spectrometry imaging at 50 micron spatial resolution. *J Am Soc Mass Spectrom.* 2017;28:2099–107.
160. Tu A, Muddiman DC. Systematic evaluation of repeatability of IR-MALDESI-MS and normalization strategies for correcting the analytical variation and improving image quality. *Anal Bioanal Chem.* 2019;411:5729–43.
161. Gilliland WM Jr., Prince HMA, Polisen A, Kashuba ADM, Rosen EP. Infrared matrix-assisted laser desorption electrospray ionization mass spectrometry imaging of human hair to characterize longitudinal profiles of the antiretroviral maraviroc for adherence monitoring. *Anal Chem.* 2019;91:10816–22.
162. Caleb Bagley M, Garrard KP, Muddiman DC. The development and application of matrix assisted laser desorption electrospray ionization: The teenage years. *Mass Spectrom Rev.* 2021:e21696.
163. He J, Sun C, Li T, Luo Z, Huang L, Song X, et al. A sensitive and wide coverage ambient mass spectrometry imaging method for functional metabolites based molecular histology. *Adv Sci (Weinh).* 2018;5:1800250.
164. Song X, He J, Pang X, Zhang J, Sun C, Huang L, et al. Virtual calibration quantitative mass spectrometry imaging for accurately mapping analytes across heterogeneous biotissue. *Anal Chem.* 2019;91:2838–46.
165. Sun C, Li T, Song X, Huang L, Zang Q, Xu J, et al. Spatially resolved metabolomics to discover tumor-associated metabolic alterations. *Proc Natl Acad Sci USA.* 2019;116:52–7.
166. Wang Z, Fu W, Huo M, He B, Liu Y, Tian L, et al. Spatial-resolved metabolomics reveals tissue-specific metabolic reprogramming in diabetic nephropathy by using mass spectrometry imaging. *Acta Pharm Sin B.* 2021;11:3665–77.
167. Yin R, Burnum-Johnson KE, Sun X, Dey SK, Laskin J. High spatial resolution imaging of biological tissues using nanospray desorption electrospray ionization mass spectrometry. *Nat Protoc.* 2019;14:3445–70.
168. Li X, Yin R, Hu H, Li Y, Sun X, Dey SK, et al. An Integrated Microfluidic Probe for Mass Spectrometry Imaging of Biological Samples*. *Angew Chem Int Ed Engl.* 2020;59:22388–91.
169. Unsuhay D, Yin R, Sanchez DM, Yang M, Li Y, Sun X, et al. High-resolution imaging and identification of biomolecules using Nano-DESI coupled to ion mobility spectrometry. *Anal Chim Acta.* 2021;1186:339085.
170. Otsuka Y, Kamihoriuchi B, Takeuchi A, Iwata F, Tortorella S, Matsumoto T. High-spatial-resolution multimodal imaging by tapping-mode scanning probe electrospray ionization with feedback control. *Anal Chem.* 2021;93:2263–72.
171. Hale OJ, Cooper HJ. Native mass spectrometry imaging of proteins and protein complexes by nano-DESI. *Anal Chem.* 2021;93:4619–27.
172. Griffiths RL, Creese AJ, Race AM, Bunch J, Cooper HJ. LESA FAIMS mass spectrometry for the spatial profiling of proteins from tissue. *Anal Chem.* 2016;88:6758–66.
173. Lamont L, Baumert M, Ogrinc Potočník N, Allen M, Vreeken R, Heeren RMA, et al. Integration of ion mobility MS(E) after fully automated, online, high-resolution liquid extraction surface analysis micro-liquid chromatography. *Anal Chem.* 2017;89:11143–50.
174. Nagy G, Veličković D, Chu RK, Carrell AA, Weston DJ, Ibrahim YM, et al. Towards resolving the spatial metabolome with unambiguous molecular annotations in complex biological systems by coupling mass spectrometry imaging with structures for lossless ion manipulations. *Chem Commun (Camb).* 2019;55:306–9.
175. Griffiths RL, Hughes JW, Abbatiello SE, Belford MW, Styles IB, Cooper HJ. Comprehensive LESA mass spectrometry imaging of intact proteins by integration of cylindrical FAIMS. *Anal Chem.* 2020;92:2885–90.
176. Hale OJ, Sisley EK, Griffiths RL, Styles IB, Cooper HJ. Native LESA TWIMS-MSI: spatial, conformational, and mass analysis of proteins and protein complexes. *J Am Soc Mass Spectrom.* 2020;31:873–9.
177. Cintron-Diaz YL, Gomez-Hernandez ME, Verhaert M, Verhaert P, Fernandez-Lima F. Spatially resolved neuropeptide characterization from neuropathological formalin-fixed, paraffin-embedded tissue sections by a combination of imaging MALDI FT-ICR mass spectrometry histochemistry and liquid extraction surface analysis-trapped ion mobility spectrometry-tandem mass spectrometry. *J Am Soc Mass Spectrom.* 2022;33:681–7.

178. Tian H, Sparvero LJ, Blenkinsopp P, Amoscato AA, Watkins SC, Bayir H, et al. Secondary-ion mass spectrometry images cardiolipins and phosphatidylethanolamines at the subcellular level. *Angew Chem Int Ed Engl.* 2019;58:3156–61.
179. Newell CL, Vorng JL, MacRae JI, Gilmore IS, Gould AP. Cryogenic OrbiSIMS localizes semi-volatile molecules in biological tissues. *Angew Chem Int Ed Engl.* 2020;59:18194–200.
180. Lim H, Lee SY, Park Y, Jin H, Seo D, Jang YH, et al. Mass spectrometry imaging of untreated wet cell membranes in solution using single-layer graphene. *Nat Methods.* 2021;18:316–20.
181. Yang M, Hu H, Su P, Thomas PM, Camarillo JM, Greer JB, et al. Proteoform-Selective Imaging of Tissues Using Mass Spectrometry. *Angew Chem Int Ed Engl.* 2022; e202200721.
182. Thomen A, Najafinobar N, Penen F, Kay E, Upadhyay PP, Li X, et al. Subcellular mass spectrometry imaging and absolute quantitative analysis across organelles. *ACS Nano.* 2020;14:4316–25.
183. Lamont L, Eijkel GB, Jones EA, Flinders B, Ellis SR, Porta Siegel T, et al. Targeted drug and metabolite imaging: desorption electrospray ionization combined with triple quadrupole mass spectrometry. *Anal Chem.* 2018;90:13229–35.
184. Olie CS, van Zeijl R, El Abdellaoui S, Kolk A, Overbeek C, Nelissen R, et al. The metabolic landscape in chronic rotator cuff tear reveals tissue-region-specific signatures. *J Cachexia Sarcopenia Muscle.* 2021;13:532–43.
185. DeLaney K, Li L. Neuropeptidomic profiling and localization in the crustacean cardiac ganglion using mass spectrometry imaging with multiple platforms. *J Am Soc Mass Spectrom.* 2020;31:2469–78.
186. Zhan L, Huang X, Xue J, Liu H, Xiong C, Wang J, et al. MALDI-TOF/TOF tandem mass spectrometry imaging reveals non-uniform distribution of disaccharide isomers in plant tissues. *Food Chem.* 2021;338:127984.
187. Föll MC, Volkman V, Enderle-Ammour K, Timme S, Wilhelm K, Guo D, et al. Moving translational mass spectrometry imaging towards transparent and reproducible data analyses: a case study of an urothelial cancer cohort analyzed in the Galaxy framework. *Clin Proteom.* 2022;19:8.
188. Debeljak Ž, Niehoff AC, Bandjak A, Mandić D, Bošnjak B, Heffer M, et al. MALDI TOF mass spectrometry imaging of blood smear: method development and evaluation. *Int J Mol Sci.* 2021;22:585.
189. Bowman AP, Blakney GT, Hendrickson CL, Ellis SR, Heeren RMA, Smith DF. Ultra-high mass resolving power, mass accuracy, and dynamic range MALDI mass spectrometry imaging by 21-T FT-ICR MS. *Anal Chem.* 2020;92:3133–42.
190. Tiquet M, La Rocca R, Kirnbauer S, Zoratto S, Van Kruining D, Quinton L, et al. FT-ICR mass spectrometry imaging at extreme mass resolving power using a dynamically harmonized ICR cell with 1w or 2w detection. *Anal Chem.* 2022;94:9316–26.
191. Becker JS, Matusch A, Wu B. Bioimaging mass spectrometry of trace elements - recent advance and applications of LA-ICP-MS: A review. *Anal Chim Acta.* 2014;835:1–18.
192. Sikora KN, Hardie JM, Castellanos-García LJ, Liu Y, Reinhardt BM, Farkas ME, et al. Dual mass spectrometric tissue imaging of nanocarrier distributions and their biochemical effects. *Anal Chem.* 2020;92:2011–8.
193. Ferey J, Larroque M, Schmitz-Afonso I, Le Maître J, Sgarbura O, Carrere S, et al. Imaging matrix-assisted laser desorption/ionization fourier transform ion cyclotron resonance mass spectrometry of oxaliplatin derivatives in human tissue sections. *Talanta.* 2022;237:122915.
194. Sans M, Feider CL, Eberlin LS. Advances in mass spectrometry imaging coupled to ion mobility spectrometry for enhanced imaging of biological tissues. *Curr Opin Chem Biol.* 2018;42:138–46.
195. Dodds JN, Baker ES. Ion mobility spectrometry: fundamental concepts, instrumentation, applications, and the road ahead. *J Am Soc Mass Spectrom.* 2019;30:2185–95.
196. Zhang C, Guo KT, Wang JY, Wang T, Wang XH, Ni K. Spatial ion density change in the electrostatic field and sensitivity improvement of ion mobility spectrometer. *Sensors Actuators B-Chemical.* 2022;354.
197. Michno W, Wehrli PM, Koutarapu S, Marsching C, Minta K, Ge J, et al. Structural amyloid plaque polymorphism is associated with distinct lipid accumulations revealed by trapped ion mobility mass spectrometry imaging. *J Neurochem.* 2022;160:482–98.
198. Helmer PO, Nordhorn ID, Korf A, Behrens A, Buchholz R, Zubeil F, et al. Complementing matrix-assisted laser desorption ionization-mass spectrometry imaging with chromatography data for improved assignment of isobaric and isomeric phospholipids utilizing trapped ion mobility-mass spectrometry. *Anal Chem.* 2021;93:2135–43.
199. Cooper-Shepherd DA, Olivos HJ, Wu Z, Palmer ME. Exploiting self-association to evaluate enantiomeric composition by cyclic ion mobility-mass spectrometry. *Anal Chem.* 2022;94:8441–8.

Springer Nature or its licensor holds exclusive rights to this article under a publishing agreement with the author(s) or other rightsholder(s); author self-archiving of the accepted manuscript version of this article is solely governed by the terms of such publishing agreement and applicable law.